Acta Pharmaceutica Sinica B 2021;11(9):2880–2899

Chinese Pharmaceutical Association
Institute of Materia Medica, Chinese Academy of Medical Sciences

Acta Pharmaceutica Sinica B

www.elsevier.com/locate/apsb
www.sciencedirect.com

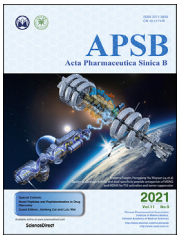

ORIGINAL ARTICLE

Lonicerin targets EZH2 to alleviate ulcerative colitis by autophagy-mediated NLRP3 inflammasome inactivation

Qi Lv[†], Yao Xing [†], Jian Liu, Dong Dong, Yue Liu, Hongzhi Qiao, Yinan Zhang[*], Lihong Hu[*]

Jiangsu Key Laboratory for Functional Substance of Chinese Medicine, Stake Key Laboratory Cultivation Base for TCM Quality and Efficacy, School of Pharmacy, Nanjing University of Chinese Medicine, Nanjing 210023, China

Received 14 October 2020; received in revised form 8 January 2021; accepted 10 February 2021

KEY WORDS

Lonicerin;
Colitis;
NLRP3 inflammasome;
Autophagy;
EZH2

Abstract Aberrant activation of NLRP3 inflammasome in colonic macrophages strongly associates with the occurrence and progression of ulcerative colitis. Although targeting NLRP3 inflammasome has been considered to be a potential therapy, the underlying mechanism through which pathway the intestinal inflammation is modulated remains controversial. By focusing on the flavonoid lonicerin, one of the most abundant constituents existed in a long historical anti-inflammatory and anti-infectious herb *Lonicera japonica* Thunb., here we report its therapeutic effect on intestinal inflammation by binding directly to enhancer of zeste homolog 2 (EZH2) histone methyltransferase. EZH2-mediated modification of H3K27me3 promotes the expression of autophagy-related protein 5, which in turn leads to enhanced autophagy and accelerates autolysosome-mediated NLRP3 degradation. Mutations of EZH2 residues (His129

Abbreviations: 3-MC, 3-methylcholanthrene; 5-ASA, 5-aminosalicylic acid; AIM2, absent in melanoma 2; ATG5, autophagy-related protein 5; ATG7, autophagy-related protein 7; ATP, adenosine triphosphate; BMDMs, bone marrow-derived macrophages; CETSA, cellular thermal shift assay; ChIP, chromatin immunoprecipitation; CHX, cycloheximide; DAI, disease activity index; DAMPs, damage-associated molecular patterns; DMSO, dimethyl sulfoxide; DSS, dextran sulfate sodium; DTT, dithiothreitol; ECL, enhanced chemiluminescent; EDTA, ethylenediaminetetraacetic acid; ELISA, enzyme-linked immunosorbent assay; EZH2, enhancer of zeste homolog 2; FBS, fetal bovine serum; H&E, hematoxylin and eosin; LPS, lipopolysaccharide; M-CSF, macrophage colony stimulating factor; MDP, muramyldipeptide; MPO, myeloperoxidase; MSU, monosodium urate crystals; NLRP3, nucleotide-binding domain-like receptors family pyrin domain containing 3; PAMPs, pathogen-associated molecular patterns; PRC2, polycomb repressive complex 2; PMA, phorbol myristate acetate; PMSF, phenylmethanesulfonyl fluoride; RMSD, root mean-square deviation; RMSF, root mean-square fluctuation; SIP, solvent-induced protein precipitation; TEM, transmission electron microscopy; UC, ulcerative colitis.

*Corresponding authors.
E-mail addresses: yinanzhang@njucm.edu.cn (Yinan Zhang), lhhu@njucm.edu.cn (Lihong Hu).
[†]These authors made equal contributions to this work.

Peer review under responsibility of Chinese Pharmaceutical Association and Institute of Materia Medica, Chinese Academy of Medical Sciences.

https://doi.org/10.1016/j.apsb.2021.03.011

and Arg685) indicated by the dynamic simulation study have found to greatly diminish the protective effect of lonicerin. More importantly, *in vivo* studies verify that lonicerin dose-dependently disrupts the NLRP3−ASC−pro-caspase-1 complex assembly and alleviates colitis, which is compromised by administration of EZH2 overexpression plasmid. Thus, these findings together put forth the stage for further considering lonicerin as an anti-inflammatory epigenetic agent and suggesting EZH2/ATG5/NLRP3 axis may serve as a novel strategy to prevent ulcerative colitis as well as other inflammatory diseases.

1. Introduction

Ulcerative colitis (UC) is a common chronic inflammatory disorder in the gastrointestinal tract. It is characterized by relapsing and diffuse mucosal inflammation, starting from the rectum and extending continuously to proximal segments of the colon[1]. Epidemiological research implicates that global incidence and prevalence of UC have been rising over time[2]. The UC patients do not suffer only from abdominal pain, bloody diarrhea, rectal bleeding and fatigue, but also from extra-intestinal manifestations such as peripheral arthritis, conjunctivitis, and body weight loss, which worsen their life quality and economic status[3]. Yet, while dysregulation of immune responses and aberrant inflammatory signals leading by genetic predisposition, destruction of epithelial barrier, and dysbacteriosis of intestinal flora have been concluded in the occurrence and development of UC, the precise etiology and etiopathogenesis of UC is still poorly understood[4]. Current non-surgical treatments including 5-aminosalicylic acid (5-ASA), glucocorticoids, immune-suppressants, biological agents and probiotics are limited by high relapse rate and different side effects[5]. Therefore, searching innovative anti-colitis drugs inspired by the latest mechanistic discovery is an urgency for the treatment of UC.

Recently, extensive studies have focused on the key role of nucleotide-binding domain-like receptors family pyrin domain containing 3 (NLRP3) inflammasome in the immune-related diseases[6]. The NLRP3 inflammasome is a multi-molecular complex that is composed of the adapter-apoptosis-associated speck-like protein containing a caspase recruitment domain (ASC) and the effector protein−caspase-1. Upon activation, NLRP3 protein interacts with ASC and pro-caspase-1 to assemble a large cytosolic complex allowing the production of cleaved caspase-1. This machinery subsequently initiates the cleavage and the secretion of pro-inflammatory cytokines interleukin 1β (IL-1β) and IL-18[7]. IL-1β accelerates inflammation by directly inducing IL-2 expression and recruiting neutrophils to augment inflammatory cascade and release other pro-inflammatory cytokines and chemokines (*e.g.*, TNF-α and IL-6)[8]; while IL-18 promotes the release of IFN-γ and accordingly enhances the proliferation of Th1 cells for further inflammatory modulation[9]. The requisite role of NLRP3 inflammasome during pathogenesis of UC has been explored on the dextran sulfate sodium (DSS) induced mouse colitis, which demonstrates that the deprivation of NLRP3 down-regulates IL-1β and IL-18 levels in the colon and ameliorates DSS-induced inflammation[10]. Many regulatory mechanisms have been identified to attenuate NLRP3 inflammasome signaling at multiple steps, including activation of nuclear factor kappa-B (NF-κB) signaling pathway, production of mitochondrial reactive oxygen species, potassium efflux and autophagy, etc. Following studies have also found that colitis is closely related with other modulators involved in the activation of atypical NLRP3 inflammasome, such as caspase 4/5/11[11]. Toward to this end, finding drug candidates targeting NLRP3 inflammasome activation and subsequent IL-1β, IL-18 production serves as an enabling anti-inflammatory strategy for the potential therapy of UC.

Natural sources traditionally used in the clinical settings have remained to be an invaluable tool for the discovery of various therapeutic agents[12]. Lonicerin is a flavonoid glycoside isolated from *Lonicera japonica* Thunb., the flower bud of which were most frequently recorded in East-Asian historical prescriptions for treating inflammatory and infectious disease[13]. A bunch of studies have demonstrated that lonicerin is one of the predominant constituents that possess anti-inflammatory and immunomodulatory activities[14,15]. Although lonicerin has recently found effective to prevent 2,4,6-trinitrobenzenesulfonic acid solution-induced colitis in rats, the mechanism related to the inactivation of NF-κB signaling pathway remains inexplicit[16]. As part of our effort to characterize active natural products[17], their unique molecular targets[18], and corresponding mechanism[19], we herein have verified the lonicerin's protective effect on DSS-induced colitis. The mechanistic study highlights lonicerin as an anti-inflammatory agent in the prevention of NLRP3−ASC−pro-caspase-1 complex assembly and colitis development.

2. Materials and methods

2.1. Chemicals and reagents

Lonicerin ($C_{27}H_{30}O_{15}$, MW: 594.5, >98% purity) was purchased from Chengdu Push Biotech (Chengdu, China); 5-ASA was purchased from Ipsen Pharma (Houdan, France); Myeloperoxidase (MPO) Kit was purchased from Jiancheng Biotech (Nanjing, China); lipopolysaccharide (LPS), phorbol myristate acetate (PMA), muramyldipeptide (MDP), adenosine triphosphate (ATP), nigericin, monosodium urate crystals (MSU) and 3-(4,5-dimethylthiazol-2-yl)-2,5-di-phenyltetrazolium bromide (MTT) were purchased from Sigma−Aldrich (St. Louis, MO, USA); DSS was purchased from MP Biomedicals (Solon, OH, USA); recombinant mouse macrophage colony stimulating factor (rmM-CSF) was purchased from Peprotech (Rocky Hill, NJ, USA); NLRP3, ASC, IL-1β, pro-caspase 1, cleaved caspase-1, cleaved IL-1β, enhancer of zeste homolog 2 (EZH2), LC3B, P62, autophagy-related gene 5 (ATG5) and ATG7 primary antibodies were purchased from Cell Signaling Technology (Danvers, MA, USA); trimethylation of lysine 27 on

histone 3 (H3K27me3) antibody was purchased from Abcam (Cambridge, UK, USA); F4/80 antibody was purchased from Wuhan Servicebio Biotech (Wuhan, China); Annexin V-FITC/PI Apoptosis Detection Kit was purchased from ThermoFisher Scientific (Waltham, MA, USA); phosphatase inhibitor cocktail, bafilomycin A1 (BafA1) and chloroquine (CQ) were purchased from Selleck Chemicals (Houston, TX, USA); RPMI 1640 medium and fetal bovine serum (FBS) were purchased from Gibco BRL (Gaithersburg, MD, USA); phenylmethanesulfonyl fluoride (PMSF), RIPA lysis buffer, Chromatin Immunoprecipitation (ChIP) Assay Kit, proteinase K and NP-40 lysis buffer were purchased from Beyotime Biotechnology (Shanghai, China); Genomic DNA Mimi Preparation Kit, QIAquick PCR Purification Kit and the EZ DNA Methylation-Gold Kit were purchased from Tiangen Biotech Co., Ltd. (Beijing, China); mouse and human IL-1β, IL-18 ELISA Kit were purchased from Dakewe Biotech (Shenzhen, China); Trizol reagent, HiScript™QRTSuperMix and AceQ™qPCR SYBR® Green Master Mix were purchased from Vazyme Biotech (Nanjing, China); Enhanced Chemiluminescent Plus Reagent Kit was purchased from Yesen Biotech (Shanghai, China); rhodamine-conjugated goat anti-rat IgG (H + L) secondary antibody, β-actin and horseradish peroxidase (HRP)-conjugated secondary antibody were purchased from Bioworld Technology (St Louis Park, MN, USA); the Entranster™-*in vivo* transfection regent was purchased from Engreen Biosystem Co., Ltd. (Beijing, China). Other chemical products used were of the analytical grade available.

2.2. Animals

The female C57BL/6 mice (weight, 20−22 g; age, 6−8 weeks) were purchased from the Comparative Medicine of Yangzhou University (Yangzhou, China). They were housed under a pathogen-free condition with the temperature of 24−25 °C and a relative humidity of 50%−55%. Animal welfare and experimental procedures were strictly carried out in accordance with the Guide for the Care and Use of Laboratory Animals (National institutes of Health, USA). The protocol was approved by the Animal Ethics Committee of Nanjing University of Chinese Medicine, Nanjing, China.

2.3. Establishment and treatment of UC

The female C57BL/6 mice were fed with 2.5% (*w*/*v*) DSS in the drinking water for 7 days followed by 3 days of recovery. To investigate the effect of lonicerin on colitis, the mice were randomly divided into the following six groups (n = 6 in each group): normal group; DSS group; lonicerin (3, 10, and 30 mg/kg) groups and 5-ASA (200 mg/kg) group.

To determine the involvement of ATG5 in lonicerin-mediated inhibition of NLRP3 inflammasome activation and attenuation of colitis, the mice were randomly divided into the following six groups (n = 6 in each group): normal group; DSS group; adeno-associated virus (AAV)-scramble shRNA group; AAV-ATG5 shRNA group; lonicerin (30 mg/kg)+AAV-scramble shRNA group; lonicerin (30 mg/kg)+AAV-ATG5 shRNA group and rapamycin (2 mg/kg) group. Prior to inducing DSS colitis, 0.1 mL of AAV-scramble (4×10^{10} vg) and AAV-ATG5 shRNA (4×10^{10} vg) were intracolonically (i.c.) administered to the mice. To determine the involvement of EZH2 in lonicerin-mediated inhibition of NLRP3 inflammasome activation and attenuation of colitis, the mice were randomly divided into the following six groups (n = 6 in each group): Normal group; DSS group; scramble plasmid group; EZH2 overexpression plasmid (10 μg) group; lonicerin (30 mg/kg)+scramble plasmid group and lonicerin (30 mg/kg)+EZH2 overexpression plasmid group. The scramble plasmid and EZH2 plasmid was mixed with equal volume Entranster *in vivo* transfection reagent, and i.c. administered 48 h prior to the onset of DSS treatment and followed by administration daily for consecutive 10 days. The intracolonical administration was carried out on the mice anaesthetized by isoflurane. Next, a soft catheter was inserted into the mouse anus at a depth of 4 cm. Scramble or EZH2 overexpression plasmid (0.1 mL) was instilled into the mouse colon *via* this catheter. The mouse was then positioned head-down for 1 min to distribute the plasmid over the colon. The lonicerin was dissolved in 0.5% CMC-Na solution and administered through gavage daily during the experiment. The normal and DSS groups received the same volume of vehicle for consecutive 10 days.

The body weight, diarrhea and rectal bleeding were measured every day, and the disease activity index (DAI) scores were calculated using the well-established system: a) body weight loss: (0 points = none; 1 points = 1%−5% loss; 2 points = 5%−10% loss; 3 points = 10%−20% loss; 4 points = over 20% loss); b) diarrhea (0 points = normal, 2 points = loose stools, 4 points = watery diarrhea); c) hematochezia (0 points = no bleeding, 2 points = slight bleeding, 4 points = gross bleeding)[20].

2.4. Histological analysis

On Day 10, the mice were sacrificed and the colons were collected. The distal colons were fixed, embedded, and sectioned for haematoxylin and eosin (H&E) staining. The histopathological scores were determined using a well-established system: a) the severity of inflammation: 0 points = none; 1 points = mild; 2 points = moderate; 3 points = severe; b) the lesion depth: 0 points = none; 1 points = mucosal layer; 2 points = submucosal layer; 3 points = muscle layer; 4 points = transmural; c) crypt damage: 0 points = none; 1 points = basal 1/3 damaged; 2 points = basal 2/3 damaged; 3 points = only surface epithelium intact; 4 points = entire crypt and epithelium lost; d) lesion range: 1 points = 1%−25%; 2 points = 26%−50%; 3 points = 51%−75%; 4 points = 76%−100%[21].

2.5. Spleen coefficient

On Day 10, the mice were sacrificed and the spleens were collected. The spleen coefficient was calculated by using Eq. (1):

$$\text{Spleen coefficient} = \text{Spleen weight (mg)}/\text{Body weight (g)} \quad (1)$$

2.6. Immunofluorescence

The distal colon of each mouse was fixed in 4% formaldehyde, embedded in O.C.T compound, frozen in liquid nitrogen, and then sectioned. Eight-micrometer-thick frozen sections of the distal colons were prepared for immunofluorescence experiments[22]. Firstly, the sections were washed with cold phosphate buffered solution (PBS) for three times and then blocked with 0.3% bovine serum albumin for 1 h at room temperature. Subsequently, the

sections were incubated with the F4/80 monoclonal antibody overnight at 4 °C. The next day, the sections were labeled with rhodamine-conjugated goat anti-rat IgG (H + L) secondary antibody for 2 h at room temperature. Lastly, the 4′,6-diamidino-2-phenylindole (DAPI) was added, and the images were carefully observed under the Olympus microscope IX73 (Tokyo, Japan).

2.7. Isolation of colonic macrophages

On Day 10, the colons were collected, carefully dissected and washed with the cold PBS for three times. Then, they were cut into 1 cm segments and placed into the RPMI 1640 medium supplemented with 1 mmol/L ethylenediaminetetraacetic acid (EDTA), 1 mmol/L dithiothreitol (DTT), 50 μg/mL gentamycin and 10% FBS. The cocktail was cultured at 37 °C with gentle shaking at 250 rpm (ThermoMixer C, Thermo Fisher, Waltham, MA, USA) for 40 min to remove the epithelial cells. After centrifugation at 1200 rpm (5424R, Eppendorf, Hamburg, Germany) for 5 min, the supernatant was removed, and the residuary colon segments were incubated with the RPMI 1640 medium supplemented with 1 mg/mL collagenase VIII, 0.1 mg/mL DNaseI, 1 mg/mL Dispase II, 50 μg/mL gentamycin and 5% FBS. Subsequently, the sample was cultured at 37 °C with gentle shaking at 250 rpm (ThermoMixer C, Thermo Fisher) for 60 min. The supernatants were collected by filtering through a nylon mesh cell strainer, and the filtered cells were layered on the Percoll solution. After centrifugation at 1200 rpm (5424R, Eppendorf) for 20 min at room temperature, the viable cells from the interphase of the Percoll solution were collected. The colonic macrophages were sorted by using F4/80 Microbeads (Miltenyi Biotec, Bergisch Gladbach, Germany).

2.8. Isolation of colonic epithelial cells

The colons were cut into 1 cm pieces and placed into the hank's balanced salt solution supplemented with 3 mmol/L EDTA and 0.5 mmol/L DTT for 1.5 h at room temperature. Subsequently, the solution was carefully removed, and the PBS solution was added to the colons. The cocktail was cultured at 37 °C with gentle shaking at 250 rpm (ThermoMixer C, Thermo Fisher) for 40 min to release the crypts from the colons. After centrifugation at 1200 rpm (5424R, Eppendorf) for 5 min, the supernatant was removed and the cells were harvested.

2.9. Cell culture

The bone marrow-derived macrophages (BMDMs) were generated from C57BL/6 mice as previously described, with minor modification. In brief, the tibiae and femurs were flushed with PBS for three times. After centrifugation at 1600 rpm (5424R, Eppendorf) for 5 min, the cells were cultured in RPMI 1640 medium supplemented with 10% FBS and 20 ng/mL rmM-CSF. The culture medium was exchanged every 3 days, and the adherent macrophages were obtained at 7 days.

The human monocytic THP-1 cell line was purchased from the Shanghai Institute of Cell Biology (Shanghai, China) and cultured in a humidified atmosphere with 5% CO_2 at 37 °C in RPMI 1640 medium supplemented with 10% FBS.

2.10. Cell viability

The viability of cells was assessed by using the MTT reagent. Briefly, 1×10^6 cells/mL BMDMs and PMA-differentiated THP-1 cells were seeded into 96-well plates, and treated with lonicerin (1, 3, 10, and 30 μmol/L) for 20 h. Afterwards, viable cell were stained with 20 μL of MTT solution (5 mg/mL) for another 4 h. Finally, the supernatant was removed, and the absorbance of formazan crystal dissolved in 150 μL dimethyl sulfoxidedmwas (DMSO) measured at 570 nm by using Microplate Reader 1500 (Thermo Fischer, Waltham, MA, USA).

2.11. Cell apoptosis

The apoptosis of cells was assessed by using the Annexin V-FITC/PI Detection Kit. Briefly, 1×10^6 cells/mL BMDMs and PMA-differentiated THP-1 cells were seeded into 6-well plates, and treated with lonicerin (1, 3, 10, and 30 μmol/L) for 24 h. Afterwards, the cells were washed with cold PBS and stained with Annexin V-FITC and PI for 30 min at room temperature. After centrifugation at 1200 rpm (5424R, Eppendorf) for 5 min, the cells were re-suspended and measured in BD FACS Calibur flow cytometer (BD, Franklin Lakes, NJ, USA). Lastly, the apoptotic cells were analyzed by using FlowJo Software (FlowJo LLC., Ashland, OR, USA).

2.12. Enzyme-linked immunosorbent assay (ELISA)

The colons were cut into 1 cm pieces and homogenate with the cold PBS. After centrifugation at 1200 rpm (5424R, Eppendorf) for 20 min at 4 °C, the supernatant was carefully collected. The levels of IL-1β and IL-18 in the supernatant and the *in vitro* culture were quantified measured by using the kits according to the manufacturer's instruments. The optical densities were read on a Microplate Reader 1500 (Thermo Fischer) at 450 and 570 nm. The levels of IL-1β and IL-18 *in vitro* culture or in colons are presented as pg/mL or pg/mg, respectively.

2.13. qPCR

The total RNA was extracted from the colons or the *in vitro* culture by using the Trizol reagent. The integrity and concentration of the extracted RNA were measured with the NanoDrop spectrophotometer (Thermo Fischer, Waltham, MA, USA). Subsequently, the total RNA was reversely transcribed to cDNA with BioRad T100 Thermal Cycler (BioRad, Hercules, CA, USA) by using HiScript™QRTSuperMix. Lastly, the PCR amplification was performed with the program: 1 cycle of 95 °C for 5 min, followed by 40 cycles of 95 °C for 10 s and 60 °C for 30 s. The primer sequences used in the experiment were listed in Table 1.

2.14. Western blotting

For total protein extraction: the cells were lysed by using the NP-40 buffer supplemented with 1 mmol/L PMSF on ice for 15 min. Subsequently, the cocktail was centrifuged at 12,000 rpm (5424R, Eppendorf) for 10 min, and the supernatants were collected. For histone extraction: the cells were lysed by using

the NP-40 buffer supplemented with 1 mmol/L PMSF on ice for 15 min and centrifuged at 12,000 rpm (5424R, Eppendorf) for 10 min. Then, the supernatants were discarded and the precipitation were re-suspended in 200 μL of 0.25 mol/L HCl on a rotator at 4 °C for overnight. Lastly, the cocktails were centrifuged at 12,000 rpm (5424R, Eppendorf) for 10 min, and the supernatants were neutralized with an appropriate volume of NaOH. The quality of the total protein and the histone was measured by using the BCA Protein Assay Kit (Beyotime Biothchnology, Shanghai, China) according to the manufacturer's instructions. The obtained protein was boiled for 10 min and then separated by using 10% sodium dodecyl sulfate-polyacrylamide gel electrophoresis. Subsequently, the discrete protein was transferred onto the polyvinylidene fluoride membranes. After blocking with 5% skim milk in Tris-buffered saline with Tween-20 for 2 h at room temperature, the membranes were incubated with the specific primary antibodies for overnight at 4 °C. The next day, the membranes were washed with Tris-

Table 1 Primers used in qPCR, DNA methylation and histone methylation.

Primer	Sequence (5′−3′)	
Actb (mouse)	Forward	CTACCTCATGAAGATCCTGACC
	Reverse	CACAGCTTCTCTTTGATGTCAC
Il6 (mouse)	Forward	CTCCCAACAGACCTGTCTATAC
	Reverse	CCATTGCACAACTCTTTTCTCA
Tnf (mouse)	Forward	ATGTCTCAGCCTCTTCTCATTC
	Reverse	GCTTGTCACTCGAATTTTGAGA
ACTB (human)	Forward	GGAAATCGTGCGTGACATT
	Reverse	CAGGCAGCTCGTAGCTCTT
IL6 (human)	Forward	CACTGGTCTTTTGGAGTTTGAG
	Reverse	GGACTTTTGTACTCATCTGCAC
TNF (human)	Forward	CTGCTGCACTTTGGAGTGATC
	Reverse	GGTTTGCTACAACATGGGCTA
Nlrp3 (mouse)	Forward	GCCGTCTACGTCTTCTTCCTTTCC
	Reverse	CATCCGCAGCCAGTGAACAGAG
NLRP3 (human)	Forward	AGAGCCCCGTGAGTCCCATTAAG
	Reverse	CGCCCAGTCCAACATCATCTTCC
Il1 (mouse)	Forward	TCGCAGCAGCACATCAACAAGAG
	Reverse	AGGTCCACGGGAAAGACACAGG
IL1 (human)	Forward	GCCAGTGAAATGATGGCTTATT
	Reverse	AGGAGCACTTCATCTGTTTAGG
Atg5 (mouse)	Forward	AGTCAAGTGATCAACGAAATGC
	Reverse	TATTCCATGAGTTTCCGGTTGA
ATG5 (human)	Forward	GATGGGATTGCAAAATGACAGA
	Reverse	GAAAGGTCTTTCAGTCGTTGTC
Atg7 (mouse)	Forward	GTGTACGATCCCTGTAACCTAG
	Reverse	GATGCTATGTGTCACGTCTCTA
ATG7 (human)	Forward	TGTATAACACCAACACACTCGA
	Reverse	GGCAGGATAGCAAAACCAATAG
M-*Atg5* promoter (mouse)	Forward	TAGTATTTGGGAGATTGAGGAATAC
	Reverse	AAATAAAAAATCCTAAAACATCGAC
U-*Atg5* promoter (mouse)	Forward	AGTATTTGGGAGATTGAGGAATATG
	Reverse	AAATAAAAAATCCTAAAACATCAAC
M-*ATG5* promoter (human)	Forward	TTTTTTGTTGGGTTAGGTAGAATAC
	Reverse	GAAACTAAACCCTACTACACTTCCG
U-*ATG5* promoter (human)	Forward	TTTTTGTTGGGTTAGGTAGAATATG
	Reverse	AAAACTAAACCCTACTACACTTCCAC
M-*Atg7* promoter (mouse)	Forward	GATTGTTATTTTAGTAATGGTGATGC
	Reverse	ACACATAAATAACTTCCTTAACGAC
U-*Atg7* promoter (mouse)	Forward	TTATTTTAGTAATGGTGATGTGG
	Reverse	ACACATAAATAACTTCCTTAACAAC
M-*ATG7* promoter (human)	Forward	TATTTCGATATTTGGTAAGGGAGAC
	Reverse	AACAAAAACATACCGAAAAAATACG
U-*ATG7* promoter (human)	Forward	TTTTGATATTTGGTAAGGGAGATGT
	Reverse	CAAAAACATACCAAAAAAATACACC
Atg5 promoter (mouse)	Forward	ACCCAGCTTCTCCTCAAC
	Reverse	TTTCTGCCACGACACTTT
ATG5 promoter (human)	Forward	CAGGAAGAAAGGGATGTT
	Reverse	CTTGCGTCAAAGCGTAGT
Atg7 promoter (mouse)	Forward	GTGATTGGTAGCCAGTTGT
	Reverse	ATGAGCGTTAGGAAGAAGG
ATG7 promoter (human)	Forward	CCCTGTGCTGCGTTTGATG
	Reverse	CTCCCTTACCAGATGTCGG

buffered saline with Tween-20 for three times and incubated with the HRP-conjugated secondary antibody for 2 h at room temperature. The binding of each antibody was visualized by using ECL according to the manufacturer's instructions. Proteins expressions were analyzed by using ImageJ software.

2.15. Co-immunoprecipitation assay

The BMDMs and the differentiated THP-1 cells were collected and washed with cold PBS for three times. Subsequently, they were lysed with RIPA lysis buffer on ice for 30 min. After centrifugation at 12,000 rpm (5424R, Eppendorf) for 10 min at 4 °C, the supernatant was carefully collected and incubated with 1 μg ASC antibody for overnight at 4 °C. The next day, the cocktails were further cultured with protein A + G agarose beads for another 4 h at room temperature. After centrifugation at 5000 rpm (5424R, Eppendorf) for 10 min, the agarose beads were washed with the lysis buffer for four times. Lastly, the immunoprecipitated proteins were separated by using 10% sodium dodecyl sulfate-polyacrylamide gel electrophoresis and captured with the specific primary antibodies.

2.16. Molecular docking

Molecular docking of lonicerin into the three-dimensional X-ray structure of EZH2 (PDB ID: 5LS6) was carried out using the docking module of the Schrödinger Maestro 2019. The three-dimensional structure of lonicerin was constructed using ChemBio 3D Ultra software (Chemical Structure Drawing Standard; Cambridge corporation, USA 2010), then it was energetically minimized by using MMFF94 with 5000 iterations and minimum RMS gradient 0.05. The protein was prepared by the protein preparation wizard of Schrödinger Maestro 2019. Waters were eliminated from the protein and the polar hydrogen was added. Receptor grids were generated using Receptor Grid Generation. The generated binding site was just the active pocket of EZH2, including several key amino acid residues. Compound lonicerin was placed during the molecular docking procedure. Types of interactions of the docked protein with ligand were analyzed after the end of molecular docking. The image files were generated using pymol 1.1.

2.17. Molecular dynamics simulation

To assess the binding stability and calculate binding free energy between lonicerin and EZH2, a 100 ns long molecular dynamics simulation was carried out, which performed with AMBER16 software package. The reference structures for protein ligand complex was taken from the predicted binding structures in molecular docking. The force field parameters for the protein and ligands were generated with Amber ff14SB and general Amber force field, respectively. The model was solvated in a truncated octahedron box of the transferable interaction potential water molecules with a margin distance of 12 Å. Sodium ions were added to neutralize the systems. The particle mesh Ewald method was used for long-range electrostatic interactions with a cutoff distance of 10 Å. Next, energy minimization was performed on the system through 2500 steps of steepest descent, followed by 2500 steps of conjugate gradients. After energy minimization, the whole system was gradually heated from 0 to 300 K for 60 ps under NVT, followed by a 600 ps NPT simulation at 1 atm, with harmonic restraints of 2 kcal/(mol·Å^2) on the complex. Finally, the 100 ns of MD production was performed at 300 K with 1.0 atm pressure. The temperature and pressure were kept constant using a Langevin thermostat and a Langevin barostat, respectively. All hydrogen atoms were constrained by the SHAKE algorithm and the time step was 2 fs. The resulting trajectories were analyzed with the AMBER16 module CPPTRAJ. The root mean square deviation (RMSD), root mean square fluctuation (RMSF) and hydrogen bonding interactions were analyzed throughout the trajectory using the CPPTRAJ module in AmberTools. The MM/GBSA method in the AMBER16 was performed to calculate the binding free energy and its position.

2.18. Bisulfite treatment and methyl-specific PCR

The genomic DNA was extracted from the BMDMs and the PMA-differentiated THP-1 cells by using the Genomic DNA Mini Preparation Kit and the DNA was purified by using a QIAquick PCR Purification Kit according to manufacturer's instructions. A total of 500 ng of *in vitro* methylated ATG5 promoter DNA was used for bisulfite modification according to the protocol provided with the EZ DNA Methylation-Gold™ Kit. This was followed by additional desalting and purification using the DNA Clean and Concentrator-5 Kit. DNA was suspended in 10 μL of RNA free water and stored at −80 °C. The corresponding methylated (M) and un-methylated (U) primers to perform methylation specific PCR on the ATG5 and ATG7 promoter were designed using Methyl Primer Express VR (Applied Biosystems, Foster City, CA, USA). A PCR reaction was performed using methylation specific PCR primer sequences in Table 1. Lastly, the PCR products were resolved in 1.5% agarose gels and then were visualized and photographed with Tanon-5200 Multi (Shanghai, China).

2.19. ChIP assay

The BMDMs and the differentiated THP-1 cells were cross-linked with 1% paraformaldehyde, and the reaction was stopped with 125 mmol/L glycine. Then, they were lysed with lysis buffer (50 mmol/L Tris pH 7.8, 10 mmol/L EDTA, and 1% SDS), and chromatin was sonicated (amplitude, 30 w; process time, 4 min; ON time, 4.5 s; OFF time, 9 s) until a range of 300 or 1000 bp was reached. Samples were diluted in dilution buffer (1% Triton, 2 mmol/L EDTA, 150 mmol/L NaCl, 20 mmol/L Tris pH 7.8) at least six times and then pre-cleared with Protein A + G Magnetic Beads. The cocktails were incubated with the H3K27me3 antibody for overnight, and then pre-cleared with Protein A + G Magnetic Beads for 1 h. The beads were sequentially washed with low salt immune complex wash buffer, high salt immune complex wash buffer, LiCl immune complex wash buffer and TE buffer. Subsequently, the beads were eluted with 0.1 mol/L $NaHCO_3$ and 1% SDS with constant agitation. The cross-linking was reverted at 65 °C for overnight, and the DNA was purified. The qPCR was performed as demonstrated above, and the primer sequences used in this assay was listed in Table 1.

2.20. Cellular thermal shift assay (CETSA)

The BMDMs and the differentiated THP-1 cells were incubated with 30 μmol/L lonicerin or DMSO for 1 h. Harvested cells were lysed using lysis buffer supplemented with pierce protease and phosphatase inhibitor. Subsequently, the soluble proteins in the supernatants were separated from cell debris by centrifuging at

16,000×*g* (5424R, Eppendorf) for 10 min at 4 °C. The supernatant was divided into fourteen aliquots and heated with various temperature (no heat, 50, 52, 54, 56, 58, 60, 62, 64, 66, 68, 70, 72 and 74 °C) *via* PCR instrument respectively, centrifuging at 16,000×*g* (5424R, Eppendorf) for 20 min at 4 °C in order to separate the soluble fraction from precipitates. The supernatants were transferred to new microtubes and analyzed by using Western blotting.

2.21. Solvent-induced protein precipitation assay (SIP)

Likewise, the cells were lysed and the supernatant was divided into fourteen aliquots. The denaturation was initiated by addition of an organic solvent mixture of acetone/ethanol/acetic acid (A.E.A) with ratio of 50:5:0.1 to reach the final percentage of organic solvent ranging from 12% to 24% (no A.E.A, 12%, 13%, 14%, 15%, 16%, 17%, 18%, 19%, 20%, 21%, 22%, 23% and 24%). Subsequently, the mixtures were equilibrated at 800 rpm (ThermoMixer C, Thermo Fisher) for 20 min at 37 °C. The supernatants were collected after the mixtures were centrifuged at 16,000×*g* (5424R, Eppendorf) for 20 min at 4 °C in order to separate the soluble fraction from precipitates. The supernatants were transferred to new microtubes and analyzed by using Western blotting.

2.22. EZH2 cloning in vector pcDNA3.1(+)

Briefly, we amplified full-length cDNA encoding human EZH2 (GeneBank: U61145.1) and mouse EZH2 (GeneBank: BC079538.1) by PCR with the specific primers including restriction sites and protecting bases (human *EZH2* Forward: 5′-GGCCGGATCCatgggccagactgggaagaaatctga-3′; human *EZH2* Reverse: 5′-GGCCGCGGCCGCtcaagggatttccatttctctttcga-3′; mouse EZH2 Forward: 5′-GGCCGGATCCatgggccagactgggaagaaatctga-3′; mouse *Ezh2* Reverse: 5′-GGCCGCGGCCGCtcaagggatttccatttctcgttcga-3′). Subsequently, the purified EZH2 products and the pcDNA3.1(+) plasmid (Invitrogen, Carlsbad, CA, USA) were digested with BamHI and NotI (New England Biolabs Inc., Ipswich, MA, USA). These enzymes have restriction site each in pcDNA3.1(+) plasmid, and the reaction was performed using 50 μL of EZH2 DNA, 6 μL of buffer, 2 μL of EcoRI (10 U/μL) and 2 μL of BamHI (10 U/μL) at 37 °C for overnight. The vector concentration was 100 ng/μL after enzyme digestion, and the digested products were purified from the gel using the Gel Extraction Kit. In order to insert EZH2 DNA into pcDNA3.1(+) vector, ligation was performed using the T4 DNA ligase. The ligation reaction contained 6 μL of pcDNA3.1(+), 3 μL of EZH2 DNA, 4 μL of T4 DNA ligase buffer and 2 μL of T4 DNA ligase (5 U/μL) and 5 μL of RNA-free water was performed at 16 °C for overnight. Subsequently, the competent cells purchased from the Vazyme (Nanjing, China) were transformed using the heat shock method, and the transformed bacteria were cultured on Luria−Bertani (LB) agar containing ampicillin 100 μg/mL. Colony-PCR was performed to confirm colonies containing the recombinant vector. Next, the recombinant vector was extracted using a QIAprep Miniprep Kit. The cloning accuracy was confirmed by sequencing.

2.23. Site-directed mutagenesis

Site-directed mutagenesis was carried out to individually or simultaneously mutate the residues Tyr111, His129, Tyr658 and Arg685 to alanine. The mutagenic primers were listed in Table 2. Subsequently, the PCR product was subcloned between the BamHI and NotI sites of the mammalian expression vector pcDNA3.1(+). All the mutations were confirmed on positive colonies by DNA sequencing.

2.24. Enzyme activity of EZH2

The EZH2 Chemiluminescent Assay Kit (Cat. #52009L) was purchased from BPS Bioscience (San Diego, CA, USA), and the enzyme activity of EZH2 was detected according to the manufacturer's instructions. Briefly, the 96-well plate was pre-coated with H3K27 substrate, *S*-adenosyl-methionine and then incubated with the EZH2 (10 ng/μL) with or without lonicerin in control. The primary antibody against methylated H3K27 HRP-labeled secondary antibody followed by addition substrate to produce chemiluminescence were used. The luminescence in untreated wells was taken as 100% activity.

2.25. Lentiviral transduction

ATG5 and scramble shRNA were purchased from the Genome Biotech (Shanghai, China). The BMDMs and THP-1 cells were seeded into the six-well plates and transfected with lentivirus-mediated shRNA according to the manufacturer's protocols. Briefly, the transduction of BMDMs and THP-1 cells were done in the presence of transduction adjuvant polybrene (10 μg/mL). The fresh medium was ex-changed after 24 h, and the transfection process lasted for another 48 h. Lastly, the cells were collected, and the transfection efficiency was detected by using the qPCR and Western blotting assays.

2.26. Statistical analysis

The data were represented as the means ± standard error of mean (SEM) of at least three independent experiments *in vitro* or six mice of each group *in vivo*. Statistical differences of means were assessed by using one-way analysis of variance (ANOVA) with the Student's *t* test between the two groups. *P* values less than 0.05 ($P < 0.05$) were considered statistically significant.

3. Results

3.1. Lonicerin ameliorates DSS-induced experimental colitis

It is well demonstrated that DSS oral administration can directly destroy the integrity of the colonic epithelial barrier, leading intestinal bacteria entry to the underneath tissues and provoking the infiltration of inflammatory cells consequently. Thus, DSS-induced colitis is a widely accepted model to resemble human clinical UC symptoms, including body weight loss, diarrhea, and rectal bleeding[23−25]. To evaluate the effect of lonicerin on colitis, the female C57BL/6 mice were challenged with 2.5% DSS for 7 days and then administered with normal drinking water for 3 days, the lonicerin (3, 10, and 30 mg/kg) and 5-ASA (200 mg/kg) were orally administrated daily for ten days. In comparison with the DSS group, lonicerin (10 and 30 mg/kg) markedly decreased the DAI scores characterized by body weight loss, diarrhea and bleeding in a dose-dependent manner (Fig. 1A and B). Colonic shortening, splenomegaly and increased MPO activity caused by DSS treatment were also improved at the given doses (Fig. 1C−E). Histological analysis indicated that lonicerin (10 and 30 mg/kg) treated mice showed remarkable alleviation on mucosal damage, infiltration of inflam-

Table 2 The primers used in site-directed mutagenesis.

Recombinant plasmid	Sequence	
EZH2 (Tyr111 mutant)	Forward 1	GGCCGGATCCatgggccagactgggaagaaatctga
	Reverse 1	agtacccataatgtattcttggtctcccc
	Forward 2	ggggagaccaagaatacattatgggtaca
	Reverse 2	GGCCGCGGCCGCtcaagggatttccatttctctttcga
EZH2 (His129 mutant)	Forward 1	GGCCGGATCCatgggccagactgggaagaaatctga
	Reverse 1	tgaaactgttttacataacattccttata
	Forward 2	tataaggaatgttatgtaaaacagtttca
	Reverse 2	GGCCGCGGCCGCtcaagggatttccatttctctttcga
EZH2 (Tyr658 mutant)	Forward 1	GGCCGGATCCatgggccagactgggaagaaatctga
	Reverse 1	aagagggaaagtgtatgataaatacatgt
	Forward 2	acatgtatttatcatacactttccctctt
	Reverse 2	GGCCGCGGCCGCtcaagggatttccatttctctttcga
EZH2 (Arg685 mutant)	Forward 1	GGCCGGATCCatgggccagactgggaagaaatctga
	Reverse 1	gggtaacaaaattcgttttgcaaatcatt
	Forward 2	aatgatttgcaaaacgaattttgttaccc
	Reverse 2	GGCCGCGGCCGCtcaagggatttccatttctctttcga

matory cells, and loss of crypts (Fig. 1F). Consistently, lonicerin (10 and 30 mg/kg) significantly abolished the distribution of F4/80$^+$ macrophages in colonic lamina propria (Fig. 1G). To further monitor the effect of lonicerin on physiological functions, the C57BL/6 mice treated with lonicerin were sacrificed after 10 days. As expected, no noticeable effect and histological changes of the organs (heart, liver, spleen, lung, kidney and colons) were observed at various doses (Supporting Information Fig. S1A−S1D). In addition, lonicerin (3, 10, and 30 mg/kg) did not alter the immune cell composition in the spleen, indicating that oral administration of lonicerin has little observed side effects (Fig. S1E). Together, these results suggest that lonicerin (10 and 30 mg/kg) showed better mitigation of DSS-induced colitis as 5-ASA did at a dose of 200 mg/kg.

3.2. *Lonicerin specifically inhibits NLRP3 inflammasome activation in colonic macrophages*

To investigate the mechanism of protective effects on murine colitis, we next assessed both mRNA and protein levels of cytokines in the collected colons. Lonicerin at the effective doses (10 and 30 mg/kg) exhibited a significant inhibition on protein expression of cleaved-caspase-1, IL-1β, and IL-18 in the colons of colitis mice (Fig. 2A and B). Given NLRP3 inflammasome projects to the maturation of these cytokines[7], the results indicate that its inactivation is crucial for the protective effect. To determine whether lonicerin-inactivated NLRP3 inflammasome was generated from macrophages rather than intestinal epithelial cells, we isolated the two types of cell lines from different mice groups. And the results showed that lonicerin only significantly suppressed the protein expression of cleaved caspase-1, IL-1β and IL-18 in the colonic macrophage (Fig. 2C and D).

Subsequently, we explored the *in vitro* effect of lonicerin on NLRP3 inflammasome activation. As shown in Fig. 2E, lonicerin (3, 10, and 30 μmol/L) significantly inhibited the protein expressions of cleaved caspase-1 and cleaved IL-1β in LPS-primed differentiated THP-1 cells and BMDMs in response to ATP, a specific NLRP3 inflammasome activator. It also suppressed secretion of IL-1β and IL-18 (Fig. 2F) without affecting the cell survival and apoptosis (Supporting Information Fig. S2A and S2B). For example, in THP-1 cells, the inhibition rate of lonicerin at 3/10/30 μmol/L against IL-1β and IL-18 were 27%/48%/74% and 21%/55%/83%, respectively. Since NLRP3 inflammasome can be activated by various endogenous and exogenous substances, we further tested whether the other NLRP3 inflammasome activators could also be prohibited consistently. The results show that the expression of cleaved caspase-1 and secretion of IL-1β were clearly diminished with irritation of both nigericin and MSU, implicating that lonicerin is a broad-spectrum inhibitor of NLRP3 inflammasome (Fig. 2G and H). To further examine the role of lonicerin involved in other inflammasomes activation, we used poly (dA:dT) to stimulate AIM2 inflammasome, MDP to NLRP1 inflammasome, and flagellin to NLRC4 inflammasome, respectively. But no inhibition was observed with gradient concentrations of lonicerin (1, 3, 10, and 30 μmol/L) on these inflammasomes (Supporting Information Fig. S3A and S3B).

3.3. *Lonicerin preferentially promotes NLRP3 degradation to disrupt assembly of NLRP3 inflammasome*

We next questioned how lonicerin regulates NLRP3 inflammasome activation. Two successive phases, priming and assembling, are reported to involve in the activation of NLRP3 inflammasome. To determine the exact phase that lonicerin takes effect, we performed co-immunoprecipitation on different parts of the NLRP3 complex and found the inhibitory concentration against NLRP3 inflammasome assembly was 3 μmol/L in both THP-1 cells and BMDMs (Fig. 3A). However, ten-fold high concentration was needed to influence the phosphorylation, nuclear transposition of P65 and *Tnf*, *Il6*, *Nlrp3* as well as *Il1* mRNA expressions when this compound was added before LPS-priming (Fig. 3B−D). These experiments suggest lonicerin at low concentration intend to retard NLRP3 inflammasome assembly. Taken this result together with a distinct observation that intact NLRP3 expression dropped with a concentration-dependent manner of lonicerin (Fig. 3E), we speculated that degradation is the primary cause for lonicerin-induced NLRP3 inflammasome inactivation. To address this hypothesis, protein synthesis pan-inhibitor cycloheximide (CHX) was used to evaluate the stability of NLRP3 in THP-1 and BMDM cells. Results in Fig. 3F show that the half-life of NLRP3 got

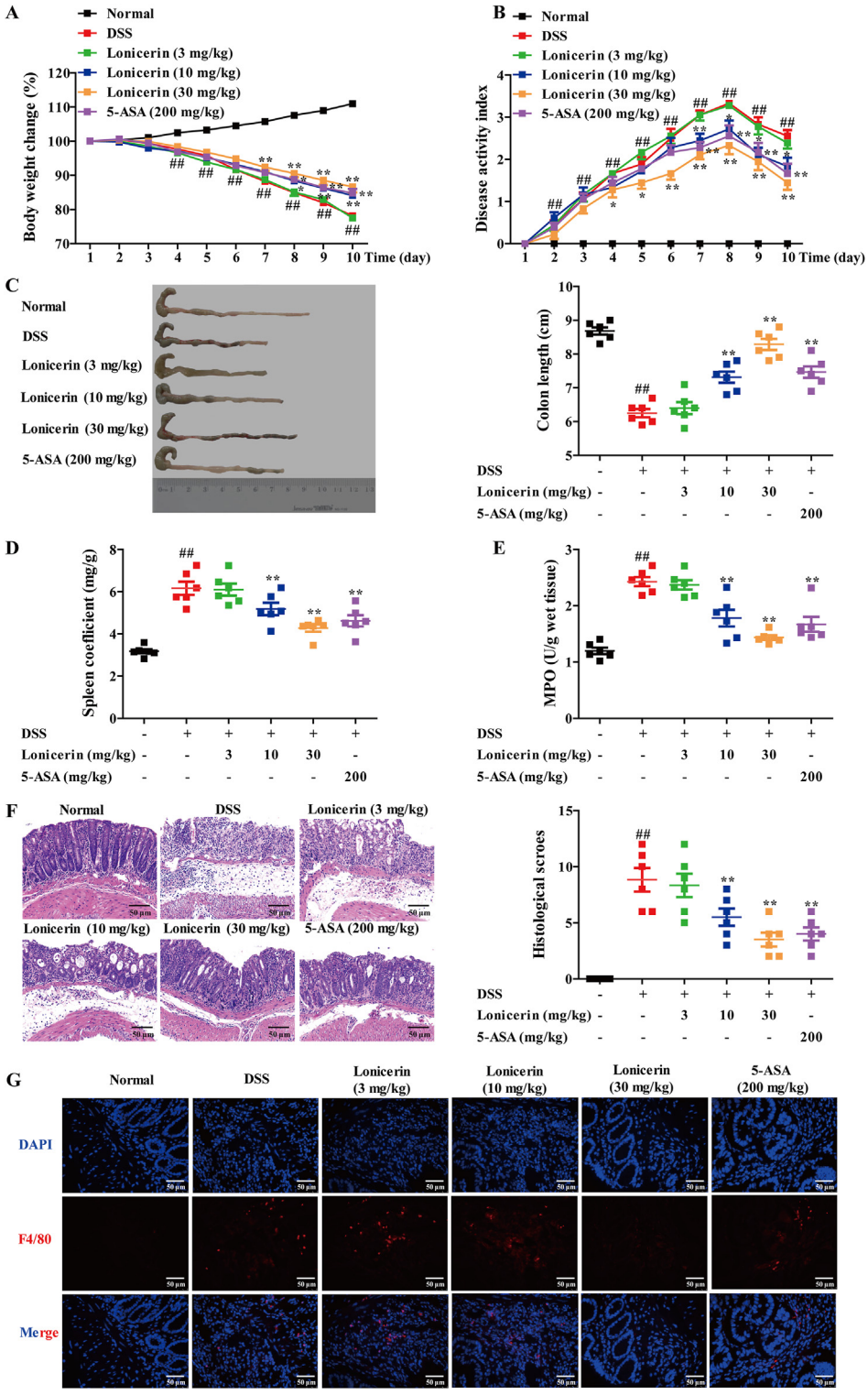

Figure 1 Lonicerin ameliorates DSS-induced experimental colitis. The C57BL/6 mice were fed with 2.5% dextran sulfate sodium (DSS) for 7 days, followed by normal drinking water for 3 days. Lonicerin (3, 10, and 30 mg/kg) and 5-ASA (200 mg/kg) were orally administrated daily for consecutive 10 days. At the end of the experiment, the mice were sacrificed, the spleens and the colons were collected. (A) The body weight change, (B) the disease activity index (DAI), (C) the colon length, (D) the spleen index, (E) the myeloperoxidase (MPO) activity in colons were measured. (F) the histopathological damage of colons was detected by using H&E staining and then scored as described in the "materials and methods" section, and the images were taken at 200 × magnification (scale bar: 50 μm). (G) the infiltration of F4/80^{+} macrophages in colonic tissue were determined by using immunofluorescence assay, and the images were taken at 200 × magnification (scale bar: 50 μm). Data are expressed as mean ± SEM of six mice in each group. $^{\#\#}P < 0.01$ *vs.* normal group; $^{*}P < 0.05$ and $^{**}P < 0.01$ *vs.* DSS group.

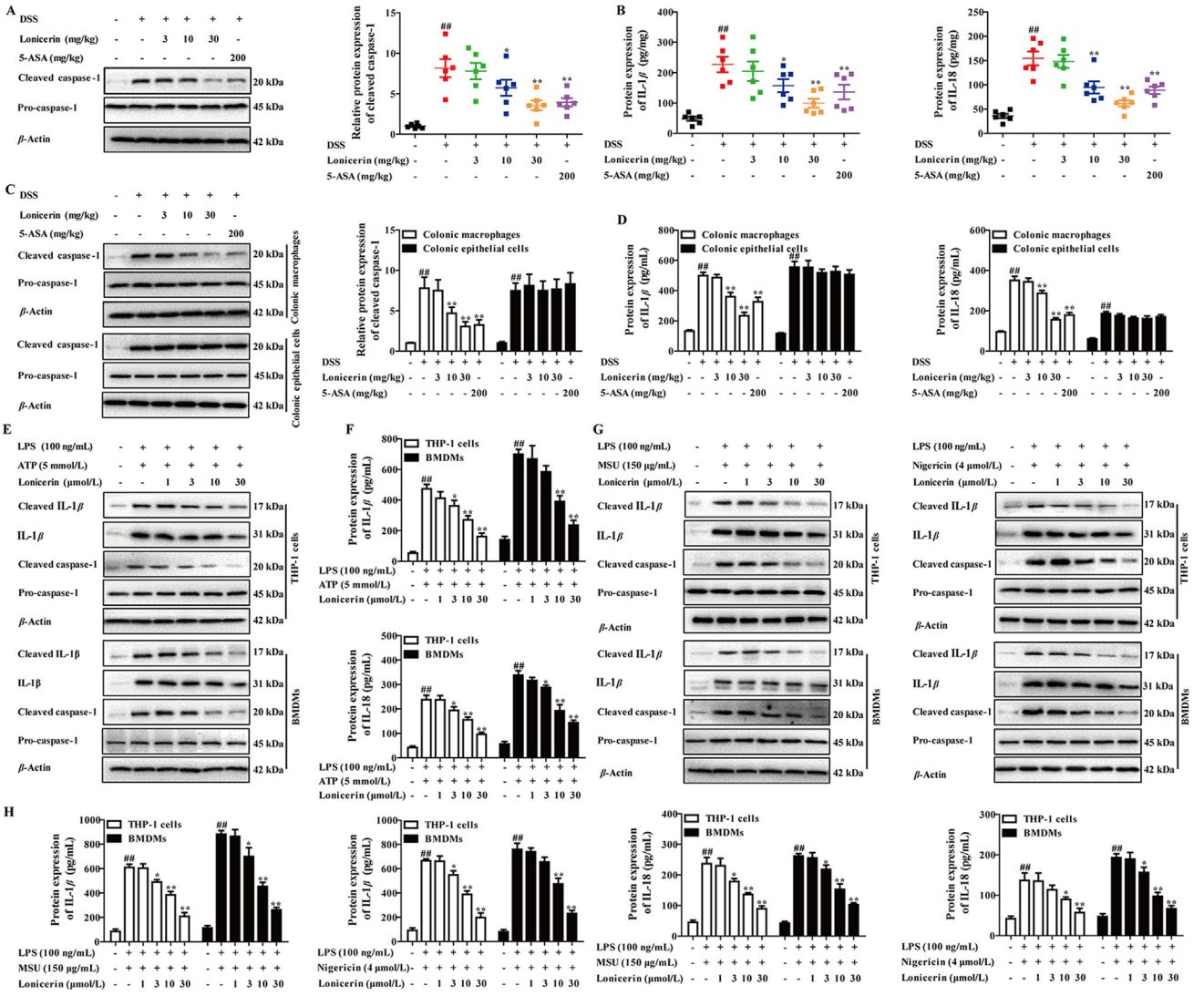

Figure 2 Lonicerin specifically inhibits NLRP3 inflammasome activation in colonic macrophages. (A−D) The mice were subjected to the DSS-induce colitis, and the colons were collected on Day 10. The protein expression of cleaved caspase-1 in colons was determined by using Western blotting assay (A); the levels of IL-1β and IL-18 in colons were detected by using ELISA (B); the immunoblot analysis of cleaved caspase-1 in colonic macrophages and epithelial cells (C); the production of IL-1β and IL-18 in colonic macrophages and epithelial cells (D). (E)−(H) The THP-1 cells (pretreated with 500 nmol/L PMA for 3 h) and BMDMs were treated with LPS (100 ng/mL) for 3 h, and then cultured with lonicerin (3, 10, and 30 μmol/L) for 6 h, followed by incubation with ATP (5 mmol/L) for 1 h, nigericin (4 μmol/L) for 3 h or monosodium urate crystals (MSU, 150 μg/mL) for 6 h. The protein expressions of cleaved caspase-1 and cleaved IL-1β were determined by using Western blotting assay (E and G); the production of IL-1β and IL-18 was analyzed by ELISA (F and H). Data are expressed as mean ± SEM of six mice in each group or at least three independent experiments. $^{\#\#}P < 0.01$ *vs*. Normal group; $^{*}P < 0.05$ and $^{**}P < 0.01$ *vs*. DSS or LPS + ATP or LPS + nigericin or LPS + MSU group.

much shorter in these cells after the treatment of lonicerin (30 μmol/L). Next, proteasome inhibitor MG-132 and lysosome inhibitor 3-mechyladenine (3-MA) were employed to probe the pathway of lonicerin-mediated NLRP3 degradation, in which the results manifested that lysosomal degradation is the decisive one (Fig. 3G and H). The degradation of NLRP3 *in vivo* was further confirmed, and the results in Fig. 3I show that lonicerin (10, 30 mg/kg) markedly decreased the protein expression of NLRP3 in colons. Collectively, these observations suggest that lonicerin triggered lysosomal degradation of NLRP3 and thus halted the activation of NLRP3 inflammasome in macrophages.

3.4. *Lonicerin enhances autophagy to inactivate NLRP3 inflammasome*

Autophagy is an evolutionarily conserved and plays a central role in the lysosomal degradation of cytoplasmic material and organelles[26]. Western blotting results, as indicated by the autophagic biomarkers LC3B−I/II and P62, displayed that lonicerin promoted autophagy or inhibited the terminal step of autophagy in a concentration-dependent manner (Fig. 4A and B). To clarify this, we treated the PMA-differentiated THP-1 cells and BMDMs with lonicerin in the presence of BafA1 or CQ. The results showed that

the above-mentioned effect of lonicerin was stronger in the presence of BafA1 and CQ, indicating lonicerin might promote autophagy (Supporting Information Fig. S4). Furthermore, an increase in LC3B-labeled vacuole formation in THP-1 and BMDMs occurred after the treatment with lonicerin (Fig. 4C). Transmission electron microscopy (TEM) showed that lonicerin markedly improved the production of autophagosomes (Fig. 4D). Notably, ATG5, which initiates the autophagic process and controls the NLRP3 inflammasome activation[27], was dramatically overexpressed (2.0/3.2/5.4 folds rises in THP-1 cells and 2.2/3.9/6.3 folds in BMDMs at 3/10/30 μmol/L lonicerin); while another autophagic initiator ATG7 did not change with the treatment of lonicerin at the same concentrations (Fig. 4E). Also, in DSS-induced colitis mice, the lonicerin (10, 30 mg/kg) significantly increased the expression of ATG5 in colons (Fig. 4F). To further validate the participation of ATG5-mediated autophagy in lonicerin-driven NLRP3 inflammasome inactivation, we used a lentiviral experiment encoding an ATG5 shRNA. As shown in Fig. 5A, the inhibitory effect of lonicerin (30 μmol/L) against NLRP3 inflammasome complex formation was reverted by ATG5 shRNA in LPS-primed differentiated THP-1 and BMDMs responsive to ATP. The protein expressions of cleaved caspase-1, cleaved IL-1β and release of IL-1β, IL-18 were reversed concomitantly (Fig. 5B and C). In contrast, the other critical process to modulate the NLRP3 inflammasome activation, mitophagy was found independent of the lonicerin-driven NLRP3 inflammasome inactivation by using an E3-ubiquitin ligase parkin shRNA (Supporting Information Fig. S5A−S5C). Finally, to confirm the above evidential findings *in vivo*, the AAV-ATG5 shRNA was intracolonically administrated into DSS-induced colitis mice. The results showed that AAV-ATG5 shRNA rescued the lonicerin (30 mg/kg)-inhibited NLRP3 inflammasome activation, testified by the increasing expression of cleaved-caspase-1 and production of IL-1β, IL-18 in colons of colitis mice (Supporting Information Fig. S6A and S6B). Furthermore, the pathological and histological improvements by lonicerin administration were eliminated by AAV-ATG5 shRNA (Fig. S6C−S6G); the decrease of macrophages infiltration in colons was also rebounded remarkably (Fig. S6H). These results further validate the statement that ATG5-mediated autophagy plays a vital role in the lonicerin-driven NLRP3 inflammasome inactivation and subsequent amelioration of DSS-induced colitis.

3.5. *Lonicerin significantly induces the expression of ATG5 and inhibits the activation of NLRP3 inflammasome through targeting EZH2*

To address whether elevated *Atg5* mRNA expression in macrophages is controlled by epigenetic factors, we initially conducted experiment on both DNA methylation and histone modification. As shown in Fig. 6A and B, no DNA methylation level change was found on the *Atg5* and *Atg7* promoter region. However, the H3K27me3 enrichment change was detected on the *Atg5* promoter but not on *Atg7* as evidenced by our findings on the mRNA levels. The gene repressive mark H3K27me3 are added to histones predominantly *via* polycomb repressive complex 2 (PRC2) and EZH2 is the core methyltransferases in the PRC2[28]. Therefore, we determined to assess whether lonicerin takes part in regulating EZH2 function. Interestingly, we failed to detect significant differences in the protein expression between the treated and untreated groups (Fig. 6C). And we proposed the hypothesis that lonicerin might directly bind to EZH2 and then inhibited its enzyme catalytic activity. Firstly, we performed a thermal shift assay to examine the interaction between lonicerin and EZH2. As shown in Fig. 6D, lonicerin enhanced the thermal stability of EZH2 by approximate 6.0 °C compared to DMSO blank. We also utilized a SIP assay to corroborate the direct interaction between lonicerin and EZH2 (Supporting Information Fig. S7). Subsequent molecular docking analysis uncovered the binding mode with an established structure of EZH2 (PDB: 5LS6, Fig. 6E). The results indicated that the aglycon of lonicerin was successfully fitted in the catalytic domain and formed multiple interactions with inside residues of EZH2, including the $\pi-\pi$ stacking between flavonoid scaffold and Tyr111/Tyr658/Tyr661, hydrogen bonding between oxygen atoms and His129/His213/Arg685, as well as an additional hydrogen bonding between sugar moiety and marginal Asn688. The enzyme catalytic activity of EZH2 in Fig. 6F confirmed that lonicerin significantly inhibited its activity.

To gain mechanistic insight of these protein-ligand interactions, we next performed a molecular dynamics simulation to evaluate the stability of the lonicerin and EZH2 complex. The RMSD and RMSF values indicated the protein−ligand complex was stabilized over a given course of simulation period (100 ns) and key residues involved in these interactions had lower fluctuation ranges than 1.0 Å (Supporting Information Fig. S8A and S8B). The calculated free energy of binding showed van der Waals (−58.89 kcal/mol) and electrostatic (−43.57 kcal/mol) contributed primarily to this protein−ligand interaction (Fig. S8C). Specifically, five residues (Tyr111, −1.6 kcal/mol; His129, −3.7 kcal/mol; His213, −1.2 kcal/mol; Tyr658, −1.6 kcal/mol; and Arg685, −5.4 kcal/mol) were recognized as essential ones to the total binding energies (−86.2 kcal/mol), in which hydrogen bonds and hydrophobic effects played dominant roles (Fig. S8D). Based on the virtual analyses, four highest-probability mutants were constructed and transfected into the THP-1 cells to verify the factual binding effect. As expected, both CETSA and SIP results showed that these mutations to alanine influenced the physical stability of EZH2 and lonicerin complex (Fig. 6G and Supporting Information Fig. S9). The stability curves of H129A and R685A had more shifting to the blank group than curves of Y111A and Y658A, indicating these two residues have enhanced affinity to the lonicerin binding.

Furthermore, we explored whether the interactions with these residues were necessary for the down-stream ATG5-mediated autophagy and NLRP3 inflammasome inactivation effect of lonicerin. The results exhibited that transfection with H129A and R685A mutation plasmid did not only greatly diminished the ATG5 level, but also attenuated lonicerin-caused inhibition of NLRP3 inflammasome activation in THP-1 cells. In contrast, Y111A and Y658A plasmids had less extent to the effect of lonicerin on ATG5-mediated autophagy and NLRP3 inflammasome inactivation (Fig. 7). Accordingly, a double mutation plasmid was constructed and transfected into THP-1 cells. The synergistic effects of H129A and R685A totally inverted the elevated expression of ATG5 and subsequent inactivation of NLRP3 inflammasome (Supporting Information Fig. S10), indicating blocking EZH2 methyltransferase activity causes a complete loss of lonicerin's protective effect.

3.6. *Lonicerin attenuates colitis through regulating the EZH2/ATG5-autophagy/NLRP3 inflammasome activation*

We finally used a DSS-induced colitis mouse model to confirm whether the protective effect of lonicerin could be attenuated by

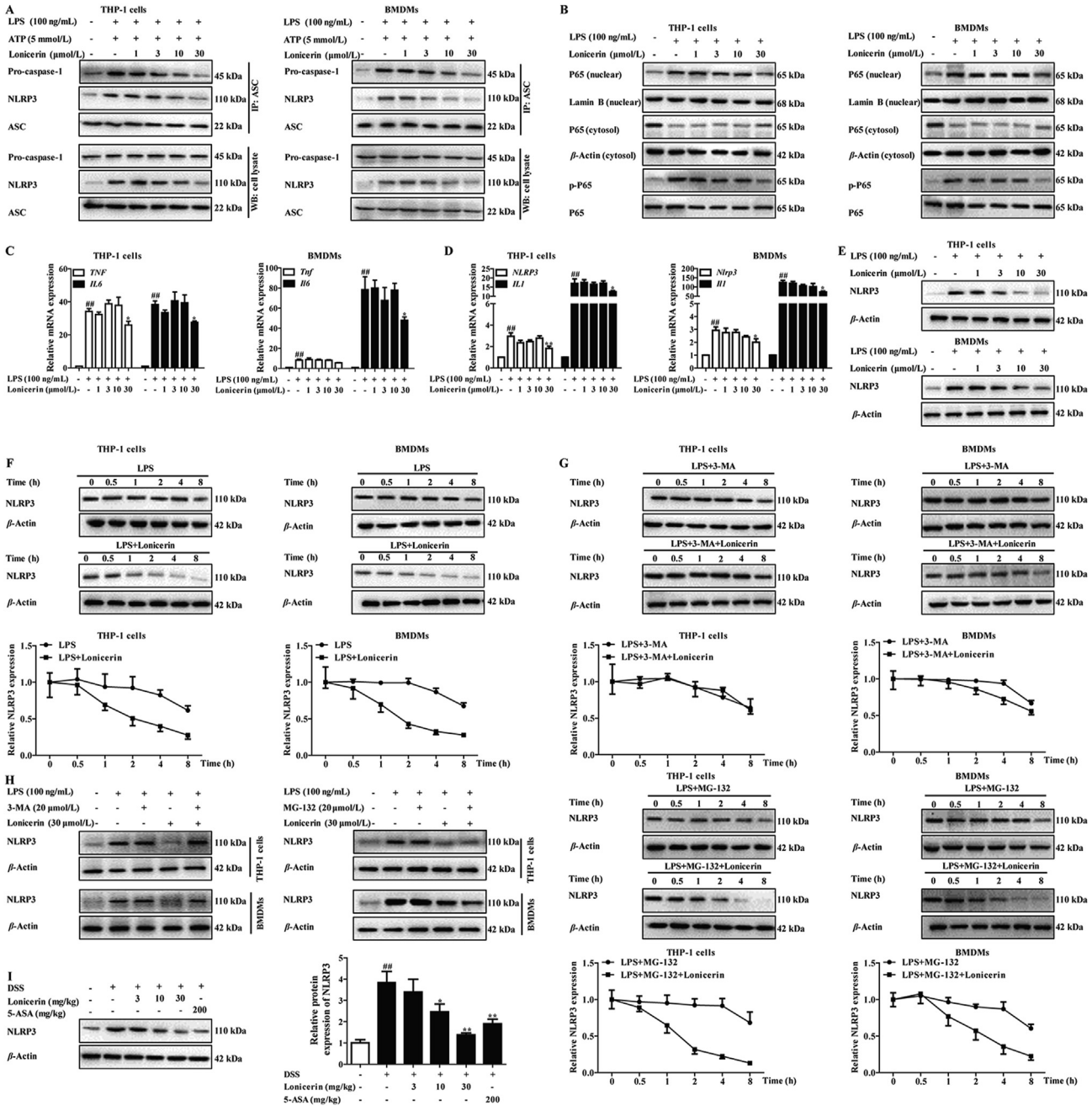

Figure 3 Lonicerin enhances NLRP3 degradation to disrupt assembly of NLRP3 inflammasome. (A) The differentiated THP-1 cells and BMDMs were treated with LPS (100 ng/mL) for 3 h, and then cultured with lonicerin (3, 10, and 30 μmol/L) for 6 h, followed by 1 h incubation with ATP (5 mmol/L). The assembly of NLRP3 inflammasome was detected by using co-immunoprecipitation assay. (B)−(D) The differentiated THP-1 cells and BMDMs were cultured with lonicerin (3, 10, and 30 μmol/L) for 6 h, and then treated with LPS (100 ng/mL) for the indicated times. The phosphorylation and nuclear transposition of NF-κB P65 were detected by using western blotting assay (B); the mRNA expressions of *Tnf*, *Il6*, *Nlrp3* as well as *Il1* were detected by using qPCR assay (C) and (D). (E) The differentiated THP-1 cells and BMDMs were treated with LPS (100 ng/mL) for 3 h, and then cultured with lonicerin (3, 10, and 30 μmol/L) for 6 h. The protein expression of NLRP3 was detected by using Western blotting assay. (F) The differentiated THP-1 cells and BMDMs were pre-treated with cycloheximide (CHX, 15 μg/mL) and LPS (100 ng/mL) for 3 h, and then cultured with lonicerin (30 μmol/L) for 6 h. The protein expressions of NLRP3 were detected by using Western blotting assay. (G and H) The differentiated THP-1 cells were pre-treated with MG-132 (20 μmol/L) or 3-methyladenine (3-MA, 20 μmol/L) and LPS (100 ng/mL), CHX (15 μg/mL) for 3 h, followed by incubation with lonicerin (30 μmol/L) for 6 h. The protein degradation and expression of NLRP3 was detected by using Western blotting assay. (I) The C57BL/6 mice were subjected to DSS-induced colitis model, lonicerin (3, 10, and 30 mg/kg) and 5-ASA (200 mg/kg) were orally administrated daily for consecutive 10 days. At the end of the experiment, the mice were sacrificed, the colons were collected and the protein expression of NLRP3 in colons was detected by using the western blotting assay. Data are expressed as mean ± SEM of at least three independent experiments or six mice in each group. $^{\#\#}P < 0.01$ *vs*. normal group; $^{*}P < 0.05$ *vs*. LPS + ATP group or DSS group.

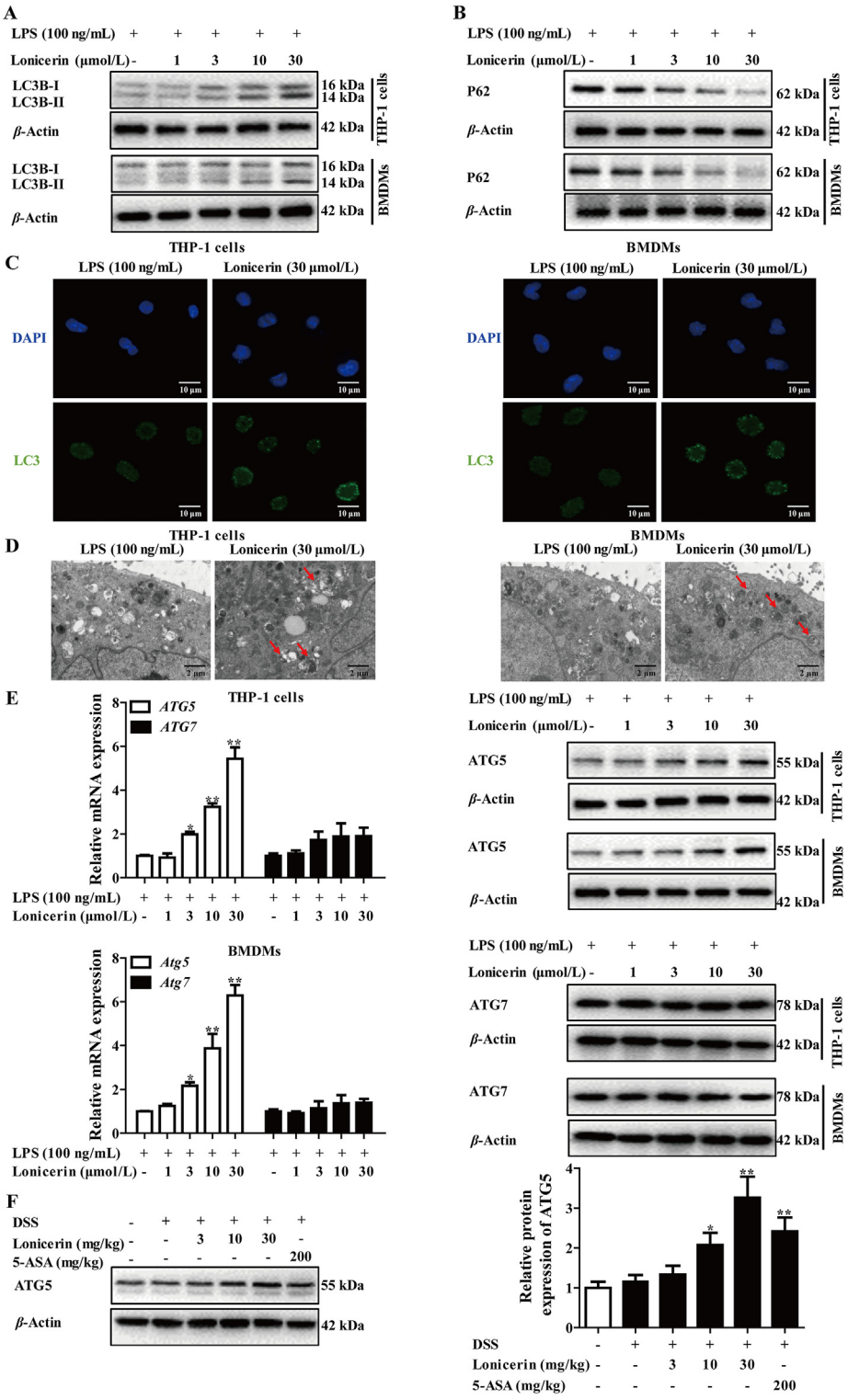

Figure 4 Lonicerin promotes autophagy in macrophages. (A)−(E) The differentiated THP-1 cells and BMDMs were pre-treated with LPS (100 ng/mL) for 3 h, and then cultured with lonicerin (3, 10, and 30 μmol/L) for 6 h. The protein expressions of LC3B-II/I (A) and P62 (B) were detected by using Western blotting assay; the LC3B dot formation was detected by immunofluorescence assay, and the images were taken at 1000 × magnification (scale bar: 10 μm) (C); the formation of autophagosome was detected by using transmission electron microscopy (scale bar: 2 μm; Red arrow, the autophagosome) (D); the levels of ATG5 and ATG7 were detected by using qPCR and Western blotting assays, respectively (E). (F) The C57BL/6 mice were subjected to DSS-induced colitis model, lonicerin (3, 10, and 30 mg/kg) and 5-ASA (200 mg/kg) were orally administrated daily for consecutive 10 days. At the end of the experiment, the mice were sacrificed, the colons were collected and the protein expression of ATG5 in colons was detected by using the Western blotting assay. Data are expressed as mean ± SEM of at least three independent experiments or six mice in each group. $*P < 0.05$ and $**P < 0.01$ *vs*. LPS group or DSS group.

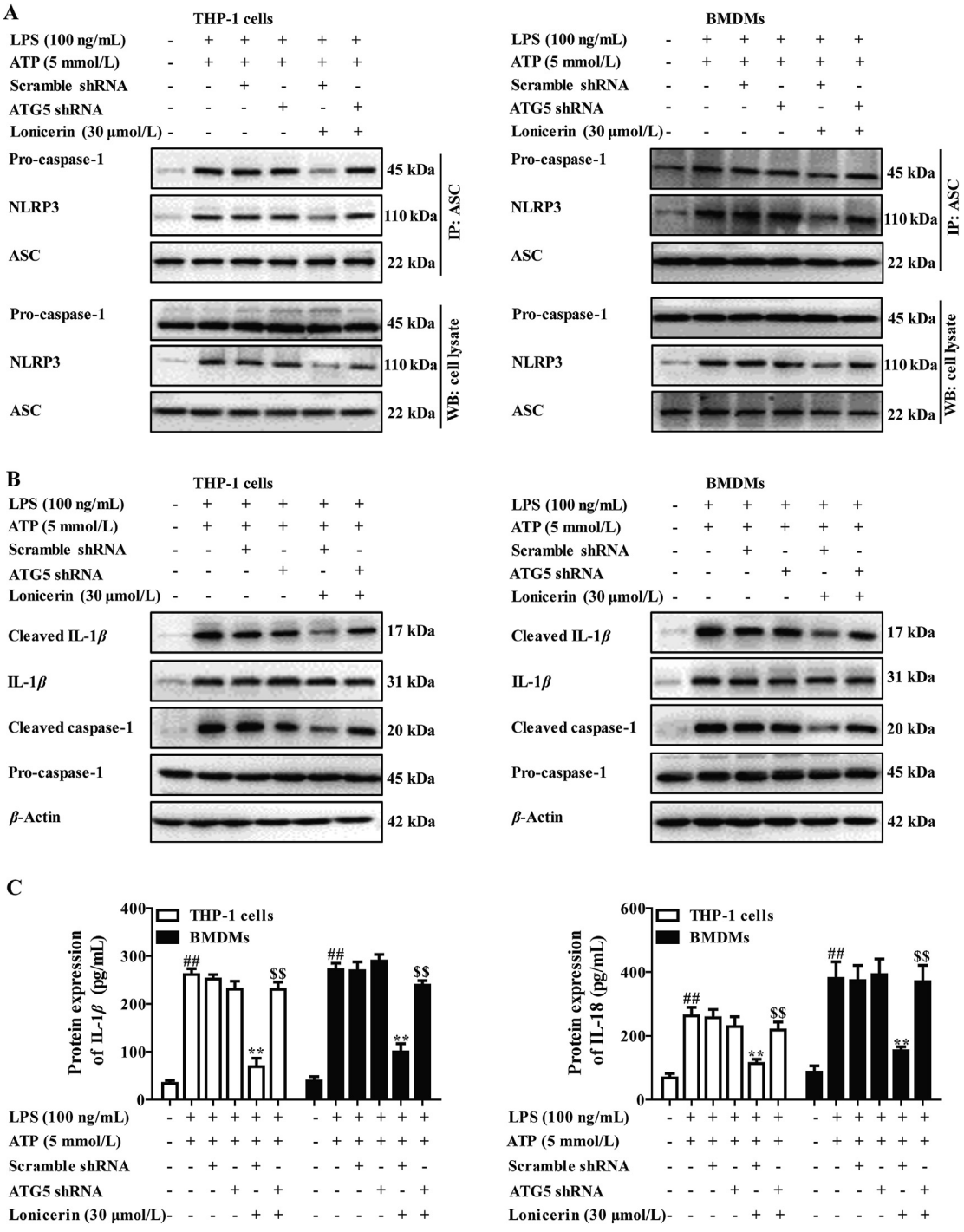

Figure 5 Lonicerin inactivates NLRP3 inflammasome *via* autophagy. The differentiated THP-1 cells and BMDMs were transfected with ATG5 shRNA and pre-treated with LPS (100 ng/mL) for 3 h, and then cultured with lonicerin (30 μmol/L) for 6 h, followed by 1 h incubation with ATP (5 mmol/L). (A) The assembly of NLRP3 inflammasome was detected by using co-immunoprecipitation assay. (B) The protein expressions of cleaved caspase-1 and cleaved IL-1β were detected by using Western blotting assay. (C) The production of IL-1β and IL-18 was detected by using ELISA. Data are expressed as mean ± SEM of at least three independent experiments. $^{\#\#}P < 0.01$ *vs*. normal group; $^{**}P < 0.01$ *vs*. LPS + ATP group; $^{\$\$}P < 0.01$ *vs*. lonicerin (30 μmol/L)+scramble shRNA group.

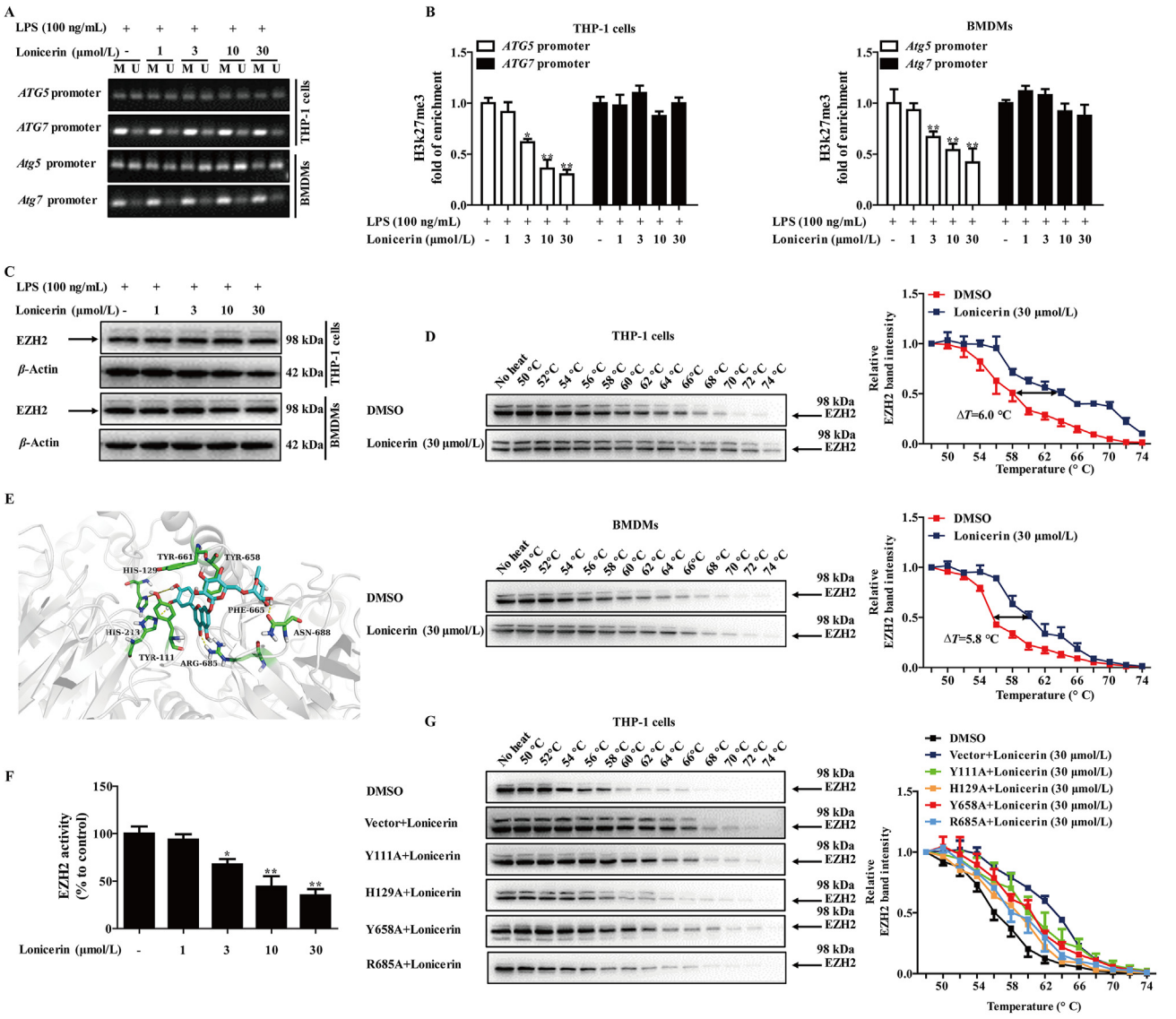

Figure 6 Lonicerin directly binds to the EZH2. (A)−(C) The differentiated THP-1 cells and BMDMs were treated with LPS (100 ng/mL) for 3 h, and then cultured with lonicerin (3, 10, and 30 μmol/L) for 6 h. The DNA methylation on *Atg5* and *Atg7* promoter was detected by using the methylation-specific PCR assay, M stands for methylated and U stands for unmethylated (A); the enrichment of H3K27me3 in *Atg5* and *Atg7* promoter was analyzed by using the chromatin immunoprecipitation assay (B); the protein expression of EZH2 was detected by using Western blotting assay (C). (D) The differentiated THP-1 cells and BMDMs were incubated with DMSO or lonicerin (30 μmol/L) for 1 h, and the whole cell lysis was suffered from CETSA assay to detect the stabilization of EZH2. (E) The interaction between lonicerin and EZH2 was detected by using molecular docking. (F) The enzyme catalytic activity of EZH2 *in vitro* was detected by using the EZH2 Chemiluminescent Assay Kit. (G) The differentiated THP-1 cells were transfected with Tyr111, His129, Tyr658, Arg685 mutation plasmids and then treated with DMSO or lonicerin (30 μmol/L) for 1 h. The interaction between lonicerin and EZH2 was detected by using CETSA assay. Data are expressed as mean ± SEM of at least three independent experiments. $^{*}P < 0.05$, $^{**}P < 0.01$ *vs*. LPS group.

the treatment of EZH2 overexpression plasmid. The model mice were intracolonically administered by EZH2 overexpression plasmid (10 μg), and the mRNA as well as protein expressions of EZH2 was significantly increased in the colons of colitis mice (Supporting Information Fig. S11). The clinical and histological results such as body weight change, DAI scores, colon length, spleen coefficients, and MPO activity showed that EZH2 plasmid significantly reversed the improvements by lonicerin administration (Fig. 8A−E). Hematoxylin and eosin (H&E) staining and immunofluorescent co-localization revealed EZH2 plasmid counteracted lonicerin's protective effects both in the colonic morphometry and macrophagic observation (Fig. 8F and G). Western blotting analysis of biomarkers ATG5, LC3B−I/II, and cleaved caspase-1 in the colonic area confirmed EZH2 plasmid

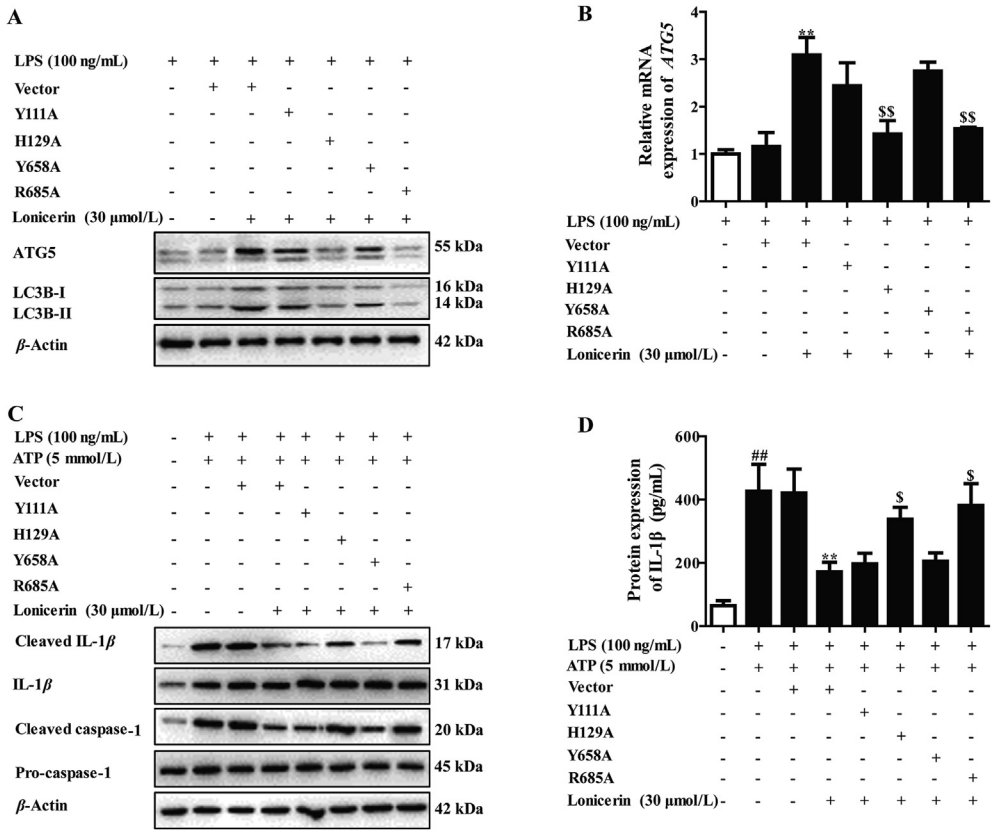

Figure 7 Lonicerin significantly induces the expression of ATG5 and inhibits the activation of NLRP3 inflammasome *via* targeting EZH2. (A and B) The differentiated THP-1 cells were transfected with Tyr111, His129, Tyr658, Arg685 mutation plasmids and pre-treated with LPS (100 ng/mL) for 3 h, and then cultured with lonicerin (30 μmol/L) for 6 h. The protein expressions of ATG5, LC3B-II/I were detected by using Western blotting assay (A); the mRNA expression of *ATG5* was detected by using qPCR assay (B). (C) and (D) The differentiated THP-1 cells were transfected with Tyr111, His129, Tyr658, Arg685 mutation plasmids and pre-treated with LPS (100 ng/mL) for 3 h, and then cultured with lonicerin (30 μmol/L) for 6 h, followed by 1 h incubation with ATP (5 mmol/L). The protein expressions of cleaved caspase-1 and cleaved IL-1β were detected by using Western blotting assay (C); the production of IL-1β was detected by using ELISA (D). Data are expressed as mean ± SEM of at least three independent experiments. $^{\#\#}P < 0.01$ *vs*. normal group; $^{**}P < 0.01$ *vs*. LPS + ATP group; $^{\$}P < 0.05$, $^{\$\$}P < 0.01$ *vs*. lonicerin (30 μmol/L)+vector group.

regressed lonicerin-enhanced ATG5-mediated autophagy and NLRP3 inflammasome inactivation (Fig. 8H and I). Collectively, these data are consistent with previous *in vitro* findings and conclude that the inhibition of EZH2 by lonicerin directly inactivates NLRP3 inflammasome and subsequently alleviates DSS-induced colitis.

4. Discussion

Ulcerative colitis is a chronic idiopathic inflammatory disorder in the colonic mucosa with an urgent need for new drugs. Recent pathogenic study of UC emphasize that abnormal immune responses and aberrant inflammatory signals are involved in its occurrence and development[4], in which the innate immune system is to sense microbial pathogens or endogenous danger signals *via* recognition of pathogen-associated molecular patterns (PAMPs) or damage-associated molecular patterns (DAMPs)[29]. Inflammasomes are a group of intracellular assembled machinery responsive to PAMPs and DAMPs and enabling to inflammatory cascade[30]. Four inflammasome receptors, including NLRP1, NLRP3, NLRC4 and AIM2 are well-characterized until now[31]. Increasing evidences have strongly supported that NLRP3 inflammasome and its signaling molecules play the key role in the pathogenesis of UC. Many studies demonstrated that activated caspase-1 is crucial for the occurrence and development of DSS-induced colitis[32], and mice deficient in caspases-1 or NLRP3 experienced alleviated clinical symptoms of colitis in comparison of the wild type[33,34]. Remarkably, the development of colitis was correlated with increased levels of IL-1β and IL-18, indicating excessive productions of these pro-inflammatory cytokines from macrophages can aggravate colitis[35]. However, the activation of NLRP3 inflammasome in epithelial cells leads to IL-18 secretion and contributes to the realization of intestinal epithelial barrier function[36]. The injection of exogenous recombinant IL-18 could ameliorate the inflammatory symptoms of DSS induced colitis[37]. The opposite roles of NLRP3 inflammasome activation prioritizes the inhibition in colonic macrophage other than intestinal epithelial cells to treat colitis. In this study, we first found that lonicerin selectively inhibited the activation of NLRP3 inflammasome in colonic macrophages and significantly alleviated colitis.

Although different stage signals involved in the activation of NLRP3 inflammasome have been investigated[38,39], NLRP3 expression is considered as a substantial factor in its related inflammatory mechanism. Several regulators have been established

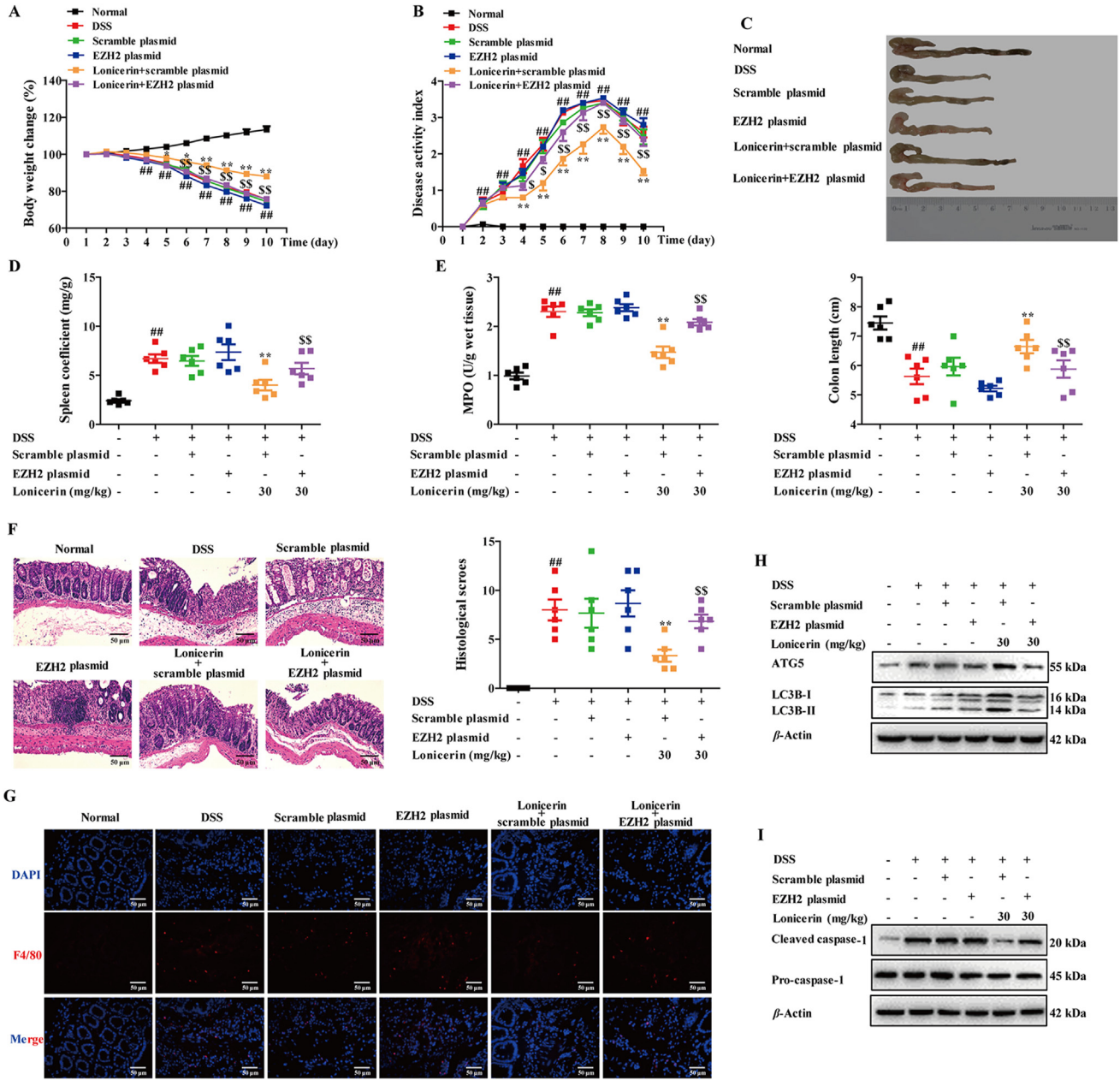

Figure 8 Lonicerin attenuates colitis through regulating the EZH2/ATG5-autophagy/NLRP3 inflammasome activation. The C57BL/6 mice were subjected to the DSS-induced colitis. The lonicerin (30 mg/kg) were orally administrated daily for consecutive 10 days. The scramble plasmid and EZH2 plasmid was mixed with equal volume Entranster *in vivo* transfection reagent, and intracolonically (i.c.) administered daily for consecutive 10 days. (A) The body weight change, (B) the disease activity index (DAI), (C) the colon length, (D) the spleen index, (E) the myeloperoxidase (MPO) activity in colons was measured. (F) The pathological changes of colons were detected by using H&E staining, and the images were taken at 200 × magnification (scale bar: 50 μm). (G) The infiltration of macrophages in colons was detected by using immunofluorescence assay, and the images were taken at 200 × magnification (Scale bar: 50 μm). (H) and (I) The protein expressions of ATG5, LC3B−I/II and cleaved-caspase-1 in colons were detected by using Western blotting assay. Data are expressed as mean ± SEM of six mice in each group; $^{\#\#}P < 0.01$ *vs.* normal group; $^{**}P < 0.01$ *vs.* DSS group. $^{\$\$}P < 0.01$ *vs.* lonicerin (30 mg/kg)+scramble plasmid group.

in eukaryotic cells, such as miR-233[40], proteasomal degradation[41], and autophagy-lysosomal degradation[42]. For example, Leishmaniasis has recently been recognized to activate autophagy-mediated degradation of NLRP3 inflammasome and subvert innate immunity by inducing the expression of ATG5[43]. Specifically, our findings discover that lonicerin treatment lead to the lysosomal degradation of NLRP3 inflammasome in both human and mouse's macrophages, as well as intriguingly remark that the autophagy process is enhanced by *Atg5* mRNA upregulation. Considering epigenetic regulation has emerged as the essential mechanism of controlling proper gene expression[44], we speculate that it may also result in the upregulation of *Atg5* mRNA

expression, which contributed to the protective effect of lonicerin on NLRP3 inflammasome activation and subsequent colitis progress.

It is well-known that histone modifications can enhance or suppress gene transcription and become increasing factors that produce aberrant immune responses in the pathogenesis of inflammatory bowel disease. EZH2 is a typical methyltranferase that controls chromatin condensation by canonically conducting tri-methylation of histone H3K27, thus functioning as a transcriptional suppressor and immunity regulator[45–49]. It is also reported that EZH2 can directly methylate target protein and activate signal transduction in the STAT3 pathway[50]. These specific functions make EZH2 inhibition and H3K27me3 modification complicated in different immune cell subsets, such as epithelial cells[45], myeloid-derived suppressor cells[46], macrophages[47], Paneth cells[48], T cells[49]. In fact, we have *in vitro* verified that EZH2 enriched tri-methylation of histone H3K27 and downregulated the mRNA level of *Atg5*. Strikingly, our DSS model with lonicerin treatment exhibits alleviation of colitis development and administration of EZH2 overexpression plasmid reverts the trend on the behalf of NLRP3 inflammasome activation, confirming the result consistency of lonicerin *in vivo*. Of note, treatment of notable EZH2 inhibitors, *e.g.*, GSK343 and GSK126, is also found to promote the generation of myeloid-derived suppressor cells from hematopoietic progenitor cells to ameliorate experimental intestinal inflammation[46]. However, the key binding residues toward lonicerin identified by our virtual and mutation studies were distinguishable from those pyridone-containing inhibitors, hence implying the binding position may result in subtle differences between histone modifications and subsequent transcriptions. In this regard, these results strongly suggest the binding profile of inhibitor determines EZH2 function as a transcriptional regulator in different subsets of immune cells.

Lonicerin is one of the major flavonoid constituents isolated from traditional Chinese medicinal herb *Lonicera japonica* Thunb., aqueous extract of which is a widely used precaution or treatment for anti-inflammatory and anti-infectious therapy. Although several groups documented the protective effects of lonicerin on different inflammatory and infection-lead inflammation diseases[13–15], their mechanism were simply ascribed to the NF-κB pathway, a universal inflammatory sensor to various stimuli. However, our data shows that the dosage needed for inhibition of NF-κB/TNF-α/IL-6 signaling pathway activation are ten folds higher than the dosage for EZH2/ATG5/NLRP3 pathway. We also notice that intracolonical administration of EZH2 plasmid largely reverses the curative effects on the NLRP3 inflammasome and DSS-induced colitis, which validates that EZH2/ATG5/NLRP3 axis is a preferential signaling pathway. It also suggests that lonicerin as well as other flavonoid congeners[51,52] from the same traditional medicinal herb are sufficient to relieve inflammation and alleviate colitis progress in colons, despite the possibilities that lonicerin may exert more regulatory characters in alternative tissues and organs cannot be excluded. Moreover, the gratifying news is that lonicerin treatment causes non-noticeable adverse effect and phenotypical changes of healthy animals in our study. Considering the herbal extracts have been used in ancient and contemporary medicinal practice with little safety concerns, we believe that lonicerin may broaden potential treatment of colitis and other inflammatory diseases with a new underlying mechanism.

5. Conclusions

Our results show that lonicerin exhibits an inhibitory effect on the activation of NLRP3 inflammasome. This mechanism is attributed to the regulation of EZH2/ATG5-mediated autophagy. This study interprets the mechanistic insight of lonicerin in the amelioration of mouse colitis and sets the stage for future consideration of EZH2/ATG5/NLRP3 axis as an innovative pathway for UC therapy.

Acknowledgments

This work was supported by the Program of the National Natural Science Foundation of China (No. 81903885, Qi Lv; No. 21877062, Yinan Zhang; No. 82073719, Lihong Hu), the program of the Jiangsu "Shuang Chuang" team (No. 20182036, Lihong Hu and Yinan Zhang, China), and the key research projects of Jiangsu Higher Education (No. 18KJA360010, Yinan Zhang, China).

Author contributions

Qi Lv, Yinan Zhang and Lihong Hu designed the study. Qi Lv, Yao Xing, Jian Liu, Dong Dong, Yue Liu, and Hongzhi Qiao performed all the experiments. In addition, Qi Lv, Yao Xing, and Yinan Zhang analyzed the data and prepared the manuscript. All the authors participated in revising the manuscript and agreed to the final version.

Conflicts of interest

The authors declare no conflicts of interest.

Appendix A. Supporting information

Supporting data to this article can be found online at https://doi.org/10.1016/j.apsb.2021.03.011.

References

1. Ungaro R, Mehandru S, Allen PB, Peyrin-Biroulet L, Colombel JF. Ulcerative colitis. *Lancet* 2017;**389**:1756–70.
2. Retnakumar SV, Muller S. Pharmacological autophagy regulators as therapeutic agents for inflammatory bowel diseases. *Trends Mol Med* 2019;**25**:516–37.
3. Neurath MF. Targeting immune cell circuits and trafficking in inflammatory bowel disease. *Nat Immunol* 2019;**20**:970–9.
4. Zundler S, Becker E, Schulze LL, Neurath MF. Immune cell trafficking and retention in inflammatory bowel disease: mechanistic insights and therapeutic advances. *Gut* 2019;**68**:1688–700.
5. de Mattos BR, Garcia MP, Nogueira JB, Paiatto LN, Albuquerque CG, Souza CL, et al. Inflammatory bowel disease: an overview of immune mechanisms and biological treatments. *Mediat Inflamm* 2015;**2015**:493012.
6. Shen HH, Yang YX, Meng X, Luo XY, Li XM, Shuai ZW, et al. NLRP3: a promising therapeutic target for autoimmune diseases. *Autoimmun Rev* 2018;**17**:694–702.
7. Jo EK, Kim JK, Shin DM, Sasakawa C. Molecular mechanisms regulating NLRP3 inflammasome activation. *Cell Mol Immunol* 2016;**13**:148–59.
8. Drummond RA, Swamydas M, Oikonomou V, Zhai B, Dambuza IM, Schaefer BC, et al. CARD9$^+$ microglia promote antifungal immunity *via* IL-1β- and CXCL1-mediated neutrophil recruitment. *Nat Immunol* 2019;**20**:559–70.

9. Deason K, Troutman TD, Jain A, Challa DK, Mandraju R, Brewer T, et al. BCAP links IL-1R to the PI3K-mTOR pathway and regulates pathogenic Th17 cell differentiation. *J Exp Med* 2018;**215**:2413−28.
10. Bauer C, Duewell P, Mayer C, Lehr HA, Fitzgerald KA, Dauer M, et al. Colitis induced in mice with dextran sulfate sodium (DSS) is mediated by the NLRP3 inflammasome. *Gut* 2010;**59**:1192−9.
11. Hsu JL, Chou JW, Chen TF, Hsu JT, Su FY, Lan JL, et al. Glutathione peroxidase 8 negatively regulates caspase-4/11 to protect against colitis. *EMBO Mol Med* 2020;**12**:e9386.
12. Newman DJ, Cragg GM. Natural products as sources of new drugs over the nearly four decades from 01/1981 to 09/2019. *J Nat Prod* 2020;**83**:770−803.
13. Shang X, Pan H, Li M, Miao X, Ding H. *Lonicera japonica* Thunb.: ethnopharmacology, phytochemistry and pharmacology of an important traditional Chinese medicine. *J Ethnopharmacol* 2011;**138**:1−21.
14. Lee SJ, Shin EJ, Son KH, Chang HW, Kang SS, Kim HP. Anti-inflammatory activity of the major constituents of *Lonicera japonica*. *Arch Pharm Res* 1995;**18**:133−5.
15. Lee SJ, Choi JH, Son KH, Chang HW, Kang SS, Kim HP. Suppression of mouse lymphocyte proliferation *in vitro* by naturally-occurring biflavonoids. *Life Sci* 1995;**57**:551−8.
16. Liu D, Yu X, Sun H, Zhang W, Liu G, Zhu L. Flos lonicerae flavonoids attenuate experimental ulcerative colitis in rats *via* suppression of NF-κB signaling pathway. *Naunyn Schmiedebergs Arch Pharmacol* 2020;**393**:2481−94.
17. Zhao H, Yang A, Liu J, Bao S, Peng R, Hu Y, et al. Chartspiroton, a tetracyclic spiro-naphthoquinone derivative from a medicinal plant endophytic streptomyces. *Org Lett* 2020;**22**:3739−43.
18. Ye Q, Zhang Y, Cao Y, Wang X, Guo Y, Chen J, et al. Frenolicin B targets peroxiredoxin 1 and glutaredoxin 3 to trigger ROS/4E-BP1-mediated antitumor effects. *Cell Chem Biol* 2019;**26**:366−77.
19. Wang J, Lv X, Xu J, Liu X, Du T, Sun G, et al. Design, synthesis and biological evaluation of vincamine derivatives as potential pancreatic β-cells protective agents for the treatment of type 2 diabetes mellitus. *Eur J Med Chem* 2020;**188**:111976.
20. Guo W, Sun Y, Liu W, Wu X, Guo L, Cai P, et al. Small molecule-driven mitophagy-mediated NLRP3 inflammasome inhibition is responsible for the prevention of colitis-associated cancer. *Autophagy* 2014;**10**:972−85.
21. Wirtz S, Popp V, Kindermann M, Gerlach K, Weigmann B, Fichtner-Feigl S, et al. Chemically induced mouse models of acute and chronic intestinal inflammation. *Nat Protoc* 2017;**12**:1295−309.
22. Shi F, Li M, Wang J, Wu D, Pan M, Guo M, et al. Induction of multiple myeloma cancer stem cell apoptosis using conjugated anti-ABCG2 antibody with epirubicin-loaded microbubbles. *Stem Cell Res Ther* 2018;**9**:144.
23. Chassaing B, Aitken JD, Malleshappa M, Vijay-Kumar M. Dextran sulfate sodium (DSS)-induced colitis in mice. *Curr Protoc Immunol* 2014;**104**:15.25.1−15.25.14.
24. Li H, Fan C, Lu H, Feng C, He P, Yang X, et al. Protective role of berberine on ulcerative colitis through modulating enteric glial cells-intestinal epithelial cells-immune cells interactions. *Acta Pharm Sin B* 2020;**10**:447−61.
25. Fan X, Ding X, Zhang QY. Hepatic and intestinal biotransformation gene expression and drug disposition in a dextran sulfate sodium-induced colitis mouse model. *Acta Pharm Sin B* 2020;**10**:123−35.
26. Eskelinen EL, Saftig P. Autophagy: a lysosomal degradation pathway with a central role in health and disease. *Biochim Biophys Acta* 2009;**1793**:664−73.
27. Liu P, Huang G, Wei T, Gao J, Huang C, Sun M, et al. Sirtuin 3-induced macrophage autophagy in regulating NLRP3 inflammasome activation. *Biochim Biophys Acta Mol Basis Dis* 2018;**1864**:764−77.
28. Jani KS, Jain SU, Ge EJ, Diehl KL, Lundgren SM, Müller MM, et al. Histone H3 tail binds a unique sensing pocket in EZH2 to activate the PRC2 methyltransferase. *Proc Natl Acad Sci U S A* 2019;**116**:8295−300.
29. Mogensen TH. Pathogen recognition and inflammatory signaling in innate immune defenses. *Clin Microbiol Rev* 2009;**22**:240−73.
30. Zhen Y, Zhang H. NLRP3 Inflammasome and inflammatory bowel disease. *Front Immunol* 2019;**10**:276.
31. Coll RC, Robertson AA, Chae JJ, Higgins SC, Muñoz-Planillo R, Inserra MC, et al. A small-molecule inhibitor of the NLRP3 inflammasome for the treatment of inflammatory diseases. *Nat Med* 2015;**21**:248−55.
32. Siegmund B, Lehr HA, Fantuzzi G, Dinarello CA. IL-1 beta-converting enzyme (caspase-1) in intestinal inflammation. *Proc Natl Acad Sci U S A* 2001;**98**:13249−54.
33. Błażejewski AJ, Thiemann S, Schenk A, Pils MC, Gálvez EJC, Roy U, et al. Microbiota normalization reveals that canonical caspase-1 activation exacerbates chemically induced intestinal inflammation. *Cell Rep* 2017;**19**:2319−30.
34. Mao L, Kitani A, Strober W, Fuss IJ. The Role of NLRP3 and IL-1β in the pathogenesis of inflammatory bowel disease. *Front Immunol* 2018;**9**:2566.
35. Perera AP, Kunde D, Eri R. NLRP3 inhibitors as potential therapeutic agents for treatment of inflammatory bowel disease. *Curr Pharm Des* 2017;**23**:2321−7.
36. Zaki MH, Lamkanfi M, Kanneganti TD. The NLRP3 inflammasome: contributions to intestinal homeostasis. *Trends Immunol* 2011;**32**:171−9.
37. Nowarski R. Epithelial IL-18 equilibrium controls barrier function in colitis. *Cell* 2015;**163**:1444−56.
38. Wang S, Lin Y, Yuan X, Li F, Guo L, Wu B. REV-ERBα integrates colon clock with experimental colitis through regulation of NF-κB/NLRP3 axis. *Nat Commun* 2018;**9**:4246.
39. Moon JS, Nakahira K, Chung KP, DeNicola GM, Koo MJ, Pabón MA, et al. NOX4-dependent fatty acid oxidation promotes NLRP3 inflammasome activation in macrophages. *Nat Med* 2016;**22**:1002−12.
40. Zhang L, Li H, Zang Y, Wang F. NLRP3 inflammasome inactivation driven by miR-223-3p reduces tumor growth and increases anticancer immunity in breast cancer. *Mol Med Rep* 2019;**19**:2180−8.
41. Song H, Liu B, Huai W, Yu Z, Wang W, Zhao J, et al. The E3 ubiquitin ligase TRIM31 attenuates NLRP3 inflammasome activation by promoting proteasomal degradation of NLRP3. *Nat Commun* 2016;**7**:13727.
42. Han X, Sun S, Sun Y, Song Q, Zhu J, Song N, et al. Small molecule-driven NLRP3 inflammation inhibition *via* interplay between ubiquitination and autophagy: implications for Parkinson disease. *Autophagy* 2019;**15**:1860−81.
43. de Carvalho RVH, Lima-Junior DS, da Silva MVG, Dilucca M, Rodrigues TS, Horta CV, et al. Leishmania RNA virus exacerbates Leishmaniasis by subverting innate immunity *via* TLR3-mediated NLRP3 inflammasome inhibition. *Nat Commun* 2019;**10**:5273.
44. Zhao M, Tan Y, Peng Q, Huang C, Guo Y, Liang G, et al. IL-6/STAT3 pathway induced deficiency of RFX1 contributes to Th17-dependent autoimmune diseases *via* epigenetic regulation. *Nat Commun* 2018;**9**:583.
45. Liu Y, Peng J, Sun T, Li N, Zhang L, Ren J, et al. Epithelial EZH2 serves as an epigenetic determinant in experimental colitis by inhibiting TNFα-mediated inflammation and apoptosis. *Proc Natl Acad Sci U S A* 2017;**114**:E3796−805.
46. Zhang X, Wang Y, Yuan J, Li N, Pei S, Xu J, et al. Targeting EZH2 histone methyltransferase activity alleviates experimental intestinal inflammation. *Nat Commun* 2019;**10**:2427.

47. Zhang X, Wang Y, Yuan J, Li N, Pei S, Xu J, et al. Macrophage/microglial EZH2 facilitates autoimmune inflammation through inhibition of SOCS3. *J Exp Med* 2018;**215**:1365−82.
48. Nakanishi Y, Reina-Campos M, Nakanishi N, Llado V, Elmen L, Peterson S, et al. Control of paneth cell fate, intestinal inflammation, and tumorigenesis by PKCλ/ι. *Cell Rep* 2016;**16**:3297−310.
49. Chen X, Cao G, Wu J, Wang X, Pan Z, Gao J, et al. The histone methyltransferase EZH2 primes the early differentiation of follicular helper T cells during acute viral infection. *Cell Mol Immunol* 2020;**17**:247−60.
50. Kim E, Kim M, Woo DH, Shin Y, Shin J, Chang N, et al. Phosphorylation of EZH2 activates STAT3 signaling *via* STAT3 methylation and promotes tumorigenicity of glioblastoma stem-like cells. *Cancer Cell* 2013;**23**:839−52.
51. Mascaraque C, Aranda C, Ocón B, Monte MJ, Suárez MD, Zarzuelo A, et al. Rutin has intestinal antiinflammatory effects in the $CD4^+$ $CD62L^+$ T cell transfer model of colitis. *Pharmacol Res* 2014;**90**:48−57.
52. Li Y, Shen L, Luo H. Luteolin ameliorates dextran sulfate sodium-induced colitis in mice possibly through activation of the Nrf2 signaling pathway. *Int Immunopharmacol* 2016;**40**:24−31.